

5-13-2021

Desalination for Sustainable Water Production with an Emphasis on Low Pressure Distillation

Jessica Vivian Savage
savagej5@my.erau.edu

Follow this and additional works at: <https://commons.erau.edu/edt>



Part of the [Energy Systems Commons](#), [Environmental Engineering Commons](#), [Heat Transfer, Combustion Commons](#), and the [Other Mechanical Engineering Commons](#)

Scholarly Commons Citation

Savage, Jessica Vivian, "Desalination for Sustainable Water Production with an Emphasis on Low Pressure Distillation" (2021). *PhD Dissertations and Master's Theses*. 595.
<https://commons.erau.edu/edt/595>

This Thesis - Open Access is brought to you for free and open access by Scholarly Commons. It has been accepted for inclusion in PhD Dissertations and Master's Theses by an authorized administrator of Scholarly Commons. For more information, please contact commons@erau.edu.

DESALINATION FOR SUSTAINABLE WATER PRODUCTION WITH AN
EMPHASIS ON LOW PRESSURE DISTILLATION

by

Jessica Vivian Savage

A Thesis Submitted to the College of Engineering Department of Mechanical
Engineering in Partial Fulfillment of the Requirements for the Degree of
Master of Science in Mechanical Engineering

Embry-Riddle Aeronautical University

Daytona Beach, Florida

May 13, 2021

DESALINATION FOR SUSTAINABLE WATER PRODUCTION WITH AN
EMPHASIS ON LOW PRESSURE DISTILLATION

by

Jessica Vivian Savage

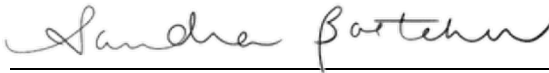
This thesis was prepared under the direction of the candidate's Thesis Committee Chair, Dr. Marc D. Compere, Associate Professor, Daytona Beach Campus, and Thesis Committee Members Dr. Sandra Boetcher, Professor, Daytona Beach Campus, and Dr. Eduardo Divo, Professor, Daytona Beach Campus, and has been approved by the Thesis Committee. It was submitted to the Department of Mechanical Engineering in partial fulfillment of the requirements for the degree of Master of Science in Mechanical Engineering.

Thesis Review Committee:



Marc D. Compere, Ph.D.

Committee Chair



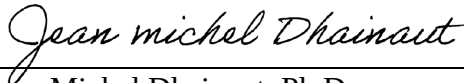
Sandra Boetcher, Ph.D.

Committee Member



Eduardo Divo, Ph.D.

Committee Member



Jean-Michel Dhainaut, Ph.D.

Graduate Program Chair,

Mechanical Engineering



Eduardo Divo, Ph.D.

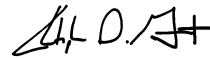
Department Chair,

Mechanical Engineering

Digitally signed by Maj Dean Mirmirani
DN: cn=Maj Dean Mirmirani, o=Embry-Riddle Aeronautical University, ou, email=mirmiram@erau.edu,
c=US
Date: 2021.06.10 13:56:36 -0400'

Maj Mirmirani, Ph.D.

Dean, College of Engineering



Christopher Grant, Ph.D.

Associate Provost of Academic Support

Date

Acknowledgements

Dr. Compere – Thank you for your technical support through my thesis and thank you for being an inspiring mentor throughout my academic career at Embry-Riddle. Through Project Haiti, Senior Design, and then the graduate program, you have shown me what it looks like to be a curious engineer, and continually reminded me that the questions worth asking are never easy to answer. Thank you for the years of meetings, mentorship, and support. I sincerely look forward to our continued friendship.

Dr. Boetcher – Thank you for your technical expertise, focus, and organization. I know that without your support, this project would not have been possible. I cannot express how much your continued belief in me has meant.

Dr. Divo – Thank you for your support through my thesis defense and thank you even more for inspiring me to pursue Mechanical Engineering in the first place. Without your guidance on my very first visit to Embry-Riddle, I would not have had the fabulous experience of going through the undergraduate and graduate Mechanical Engineering programs at ERAU. In one small moment, you absolutely impacted the rest of my career.

To my family, my teammates, coaches, Jennifer, 17106, and The Puppies – Thank you for the words of encouragement and belief in my ability to complete this project. There were definitely times when completing this project felt impossible, but all of you supported me and believed in me. Without that support, I am sure I would never have made it to this point. Thank you so much, my dear friends.

Abstract

Researcher: Jessica Vivian Savage

Title: Desalination for Sustainable Water Production with an Emphasis on Low Pressure Distillation

Institution: Embry-Riddle Aeronautical University

Degree: Master of Science in Mechanical Engineering

Year: 2021

Freshwater resources depletion is a growing concern. This freshwater scarcity motivates research into seawater desalination as a means for alleviating the stresses on water demands. The primary methods of desalination include filtration and distillation. This paper explores the potential energy savings of vacuum distillation for seawater desalination to reduce the amount of energy needed to achieve phase change.

Depending on the vacuum boiler design, the vaporization mechanism may be boiling, evaporation, or cavitation. There is very little literature on cavitation that involves mass transfer, so cavitation is not developed here. This thesis focuses on standard models for boiling and evaporation at STP then explores the potential for these models to represent vacuum desalination. To model the transition to vacuum, the model parameters are changed for boiling. The resulting fresh water mass outputs are presented. The purpose is to determine if low pressure conditions are favorable to producing freshwater compared to STP.

The final output of this thesis is a proposed algorithm for estimating fresh water mass transfer from a solar vacuum distillation process as a function of heat and electrical inputs.

Table of Contents

Thesis Review Committee.....	ii
Acknowledgements	iii
Abstract.....	iv
List of Figures.....	xi
List of Tables	xiv
1 Problem Introduction.....	1
1.1 Desalination Techniques.....	4
1.2 Low Pressure Desalination Potential.....	5
1.3 Significance of the Study.....	6
1.4 Statement of the Problem	7
1.5 Purpose Statement	9
1.6 Thesis statement	10
1.7 Limitations and Assumptions.....	10
1.8 Thesis Document Organization	11
1.9 Definitions of Terms.....	11
1.10 List of Acronyms	13
2 Methods of Desalination.....	15
2.1 Desalination Methods.....	16

2.2	Biological Filtration - Avian.....	16
2.3	Oscillatory Species Separation.....	18
2.4	Graphene Filtration.....	19
2.5	Electrodialysis	20
2.6	Geothermal Desalination	21
2.7	Freezing Desalination.....	23
2.8	Seawater Greenhouse	24
2.9	Solar Still	26
2.10	Distillation at STP	29
2.10.1	Multi-Stage Flash Distillation	32
2.10.2	Multi-Effect Distillation	34
2.10.3	Mechanical Vapor Compression	35
2.11	Reverse Osmosis.....	36
2.12	Conclusion.....	36
3	Reverse Osmosis.....	41
3.1	History of Reverse Osmosis	41
3.2	How RO Works	43

3.2.1	System Level Structure.....	43
3.2.2	Membrane Level Structure.....	44
3.3	Summary of the benefits and drawbacks of Reverse Osmosis.....	46
3.4	Reverse Osmosis Rig at Embry-Riddle.....	48
3.4.1	Project Goals and Requirements.....	48
3.4.2	Schematics.....	49
3.4.3	SolidWorks Rendition.....	50
3.4.4	Final Build.....	51
3.5	Tampa Desalination Plant.....	52
3.6	Conclusion.....	55
3.7	Recommendations for Future Work in RO.....	55
4	Vacuum Distillation.....	57
4.1	Characteristics of boiling in standard pressure systems.....	57
4.1.1	Subcooled boiling.....	57
4.1.2	Effect of wall thickness on heat flux.....	58
4.1.3	Activation site patterns.....	59
4.1.4	Maximizing heat transfer at the heated surface.....	59

4.2	Characteristics of boiling in low pressure systems.....	60
4.2.1	Pool boiling at low pressure	60
4.2.2	Heat transfer characteristics.....	60
4.2.3	Bubble dynamics	61
4.2.4	Surface finish and activation sites	64
4.2.5	Non-homogeneity	65
4.3	Mass transfer at standard pressure.....	66
4.3.1	HVAC Applications	66
4.4	A Laboratory Example Illustrating the Complexity of Low Pressure Phase Change.....	67
4.5	Summary.....	69
4.6	Thesis statement	69
5	Boiling Models and Predictions	70
5.1	Conventional Mass Transfer Models.....	70
5.1.1	Pool Boiling at Standard Pressure	70
5.1.2	Low-Pressure Pool Boiling Model	75
5.1.3	Evaporative Cooling; Heat and Mass Transfer Model in HVAC.....	78

5.1.4	Evaporative Mass Transfer Model at Standard Pressure.....	82
5.2	Creating a Comprehensive Model for Low Pressure.....	84
5.3	Theoretical Model Implementation Numerically	84
5.3.1	Assumptions	85
5.3.2	Limitations of the Model	85
5.3.3	Mathematical Model Parameters	86
5.3.4	Model Prediction Results for Properties of water from 0 to 374 degrees .	87
5.4	Numerical Model Results	88
5.4.1	Model Validation Points.....	92
5.4.2	Estimated Energy Savings for Low Pressure Distillation	94
6	Concluding Remarks & Future Work.....	96
6.1	Concluding Remarks	96
6.2	Future Work.....	97
6.2.1	Design of a physical testing apparatus	97
6.2.2	Scalability	98
6.2.3	Standard Test Procedure.....	99
6.2.4	Experimental Verification of Rohsenow at Low Pressure	99

6.2.5 Energy trade off: drawing vacuum versus thermodynamic energy savings
100

7 Referencess.....101

List of Figures

Figure 1: Global water scarcity estimates in 2019 (Sengupta & Cai, 2019).	2
Figure 2: Global use of fresh water based on data from UN-Water (Pugsley, Zacharopoulos, Mondol, & Smyth, 2016).....	3
Figure 3: Global use of fresh water based on data from UN-Water (Pugsley, Zacharopoulos, Mondol, & Smyth, 2016).....	7
Figure 4: Graphical display of volume of water produced across the globe (Jones, Qadir, van Vliet, Smakhtin, & Kang, 2019).	15
Figure 5: Taxonomy of the methods of desalination outlined in this paper.	16
Figure 6: Image of the salt removal mechanism in marine birds (Lovette & Fitzpatrick, 2017).....	17
Figure 7: Representation of the 2D material, graphene (Boretti, et al., 2018).	20
Figure 8: Geothermal system utilized for energy production (REVE, 2013).....	22
Figure 9: Schematic of a seawater greenhouse setup for an arid climate (Cho, 2011).	25
Figure 10: The test and demonstration center for the seawater greenhouse setup in Jordan (Sahara Forest Project, n.d.).	26
Figure 11: Schematic of solar dome (How Solar Stills Work, 2012).....	27
Figure 12: Image of a solar dome (How Solar Stills Work, 2012).....	27
Figure 13: Overview of a solar trough (Ahsan & Fukuhara, 2010).	28
Figure 14: Side view of a solar trough setup (Ahsan & Fukuhara, 2010).....	28

Figure 15: Basic form of a basin-type solar still (Ahsan & Fukuhara, 2010).	29
Figure 16: Schematic of an example of the system setup that inspired this study.	30
Figure 17: The figure above shows the relationship between temperature and pressure regarding the phase change of water.	31
Figure 18: Schematic of MSF unit (Al-Karaghoul, Kazmerski, & (NREL), 2013).....	32
Figure 19: MED unit setup (Al-Karaghoul, Kazmerski, & (NREL), 2013).....	34
Figure 20: Schematic of a vapor compression unit (Al-Karaghoul, Kazmerski, & (NREL), 2013).....	35
Figure 21: Widely accepted stages for TRL (TWI, 2021).....	37
Figure 22: Development of asymmetric RO membranes (Lee, Arnot, & Mattia, 2010)...	41
Figure 23: Shown above is the setup for the reverse osmosis unit in the Energy Systems Laboratory at ERAU.....	43
Figure 24: Structure of a typical spiral-wound membrane (A Perspective on Reverse Osmosis Water Desalination: Quest for Sustainability).	45
Figure 25: Shows the size of RO pores compared to salt, bacteria, and viruses (PureRO USA, 2019).....	46
Figure 26: Electrical schematic for the ERAU test rig.....	49
Figure 27: Schematic of the entire system.....	49
Figure 28: 3D Model of the RO Test Rig, done in SolidWorks.....	50
Figure 29: Physical RO Test Rig located in the Energy Systems Laboratory at ERAU...51	

Figure 30: Tampa Bay Desalination unit pumps, courtesy of Tampa Bay Water.....	52
Figure 31: Tampa Bay Desalination plant reverse osmosis units.....	53
Figure 32: Water production totals in 2017. *All water sent to Tampa Bay Water.....	54
Figure 33: Water production totals in 2018. *All water sent to Tampa Bay Water.....	54
Figure 34: Illustrates the progression of bubble dynamics of water and cyclohexane at various pressures (Michaie, Rulliere, & Bonjour, 2019).....	62
Figure 35: Schematic of a direct evaporative cooler (Fouda & Melikyan, 2010).....	67
Figure 36: Shown above is a laboratory experiment of low-pressure vaporization. Inside the sealed vacuum chamber is a glass jar with warmed water inside of it.	68
Figure 37: Typical boiling curve for water at 1atm (Faghri & Zhang, 2006).	72
Figure 38: Schematic of evaporative cooler analysis (Fouda & Melikyan, 2010).	79
Figure 39: Boiling curve for water at 1atm (Faghri & Zhang, 2006).....	89
Figure 40: Heat transfer as a function of excess temperature.....	90
Figure 41: Mass transfer of fresh water vapor as a function of excess temperature.	91
Figure 42: Numerical verification of the math within the model.	92
Figure 43: The blue circle represents a physical experimental data point. The blue X shows the predicted point based on the heater surface area.	93
Figure 44: Mass transfer of fresh water vapor as a function of heat transfer.	94
Figure 45: Demonstration of how low-pressure distillation saves energy by reducing the sensible heat needed for the system.....	95

List of Tables

Table 1.1: Summary of desalination methods in both energy consumption, TRL and applicability (Al-Karaghoul, Kazmerski, & (NREL), 2013).....	38
Table 5.1: Surface tension at the liquid-vapor interface of water (Cengel & Ghajar, 2016).....	73
Table 5.2: Values of C and n for various surface-fluid combinations (Bergman, Incropera, DeWitt, & Lavine, 2011).....	74
Table 5.3: Values of Fresh Water.....	86

Chapter I

1 Problem Introduction

Water security is reliable access to clean water and is critical for human, economic, and ecological world health. According to the World Water Assessment Programme (WWAP), it is estimated that globally, about 30 percent of the population lives in water-stressed areas, or in places where more than 40 percent of the available freshwater is being drawn at rates faster than it can be replenished (Vorosmarty, Green, Salisbury, & Lammers, 2000). Furthermore, it is estimated that by the end of this decade, that number will increase, with estimates stating that over 50 percent of the global population will be living in water-stressed conditions (WWAP (UNESCO World Water Assessment Programme), 2019). Climate change is altering weather patterns that affect the availability of freshwater (Hanasaki, et al., 2013). The population is expected to grow from about 7 billion currently to a maximum of 12.5 billion by 2050, putting even more stress on water resources (Department of International Economic and Social Affairs, 1992). Additionally, as manufacturing and technology continue to increase in both developed and developing countries, the need for water that is used for cooling and production in these processes will be increasing (WWAP (UNESCO World Water Assessment Programme), 2019). With so many demands on water resources, as shown Figure 2 below, in it is imperative that scientists and engineers explore alternative solutions to water supply. In the United Nation's Sustainable Development Goals, they have listed "Clean Water and Sanitation"

as goal number 6, stating that the goals it to “ensure availability and sustainable management of water and sanitation for all” (United Nations, 2020).

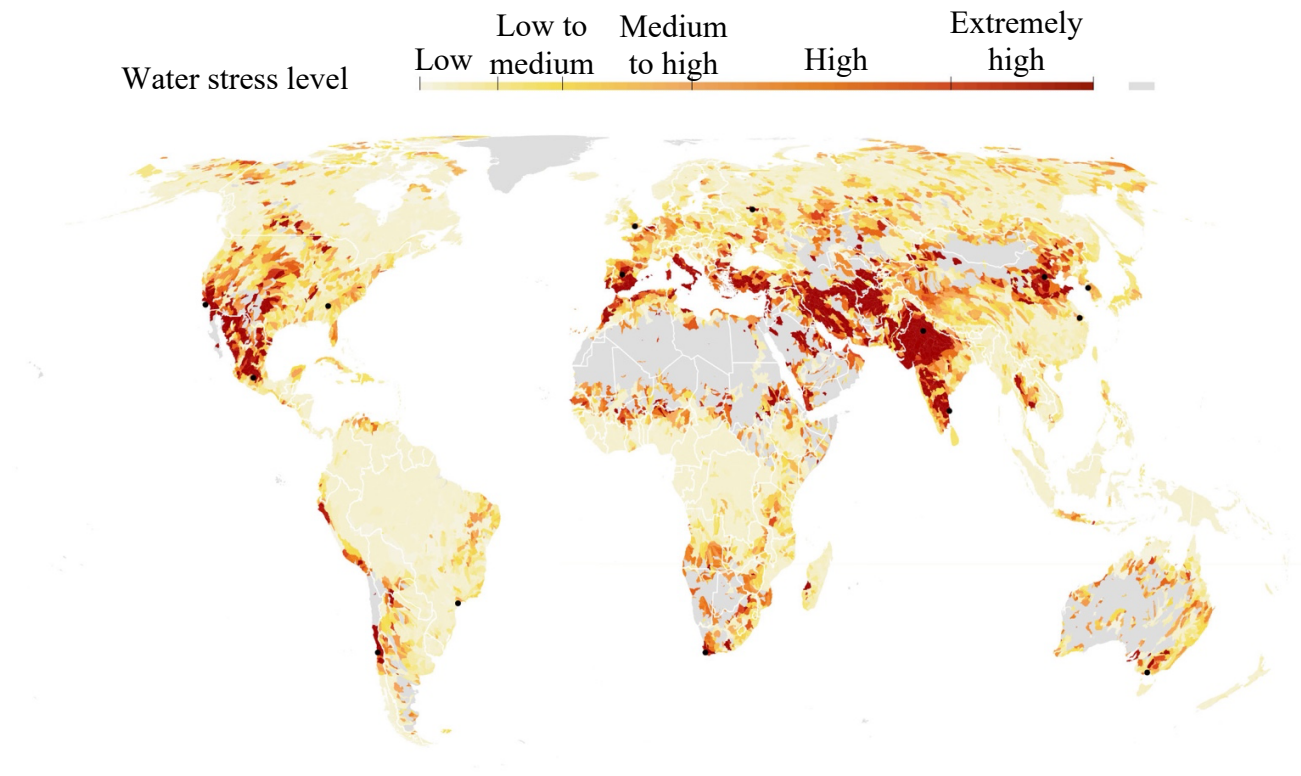


Figure 1: Global water scarcity estimates in 2019 (Sengupta & Cai, 2019).

Desalination offers a means of harvesting fresh water from saltwater resources. Over 97% of the water on earth is saltwater, while less than a half percent is readily available freshwater (Cohen, 2017; Shiklomanov, 1993). Approximately 1.75% of the water in the

world is trapped in glaciers and ice caps, 1.69% is stored as groundwater, and about 0.014% of global water resources are fresh surface water (Cohen, Semiat, & Rahardianto, 2017).

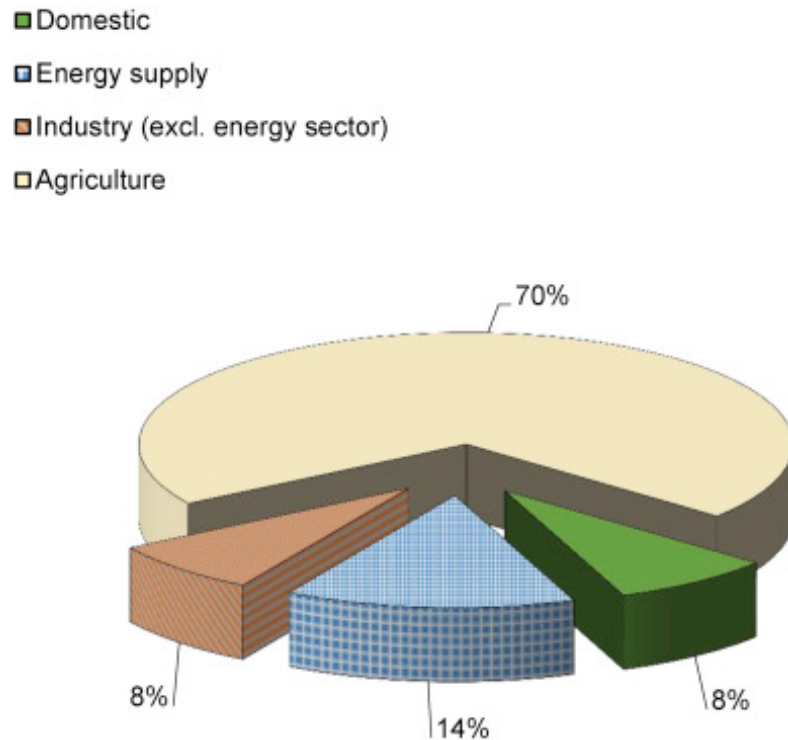


Figure 2: Global use of fresh water based on data from UN-Water (Pugsley, Zacharopoulos, Mondol, & Smyth, 2016).

With easily accessible surface fresh water as the smallest sector of earth's water stores, in addition to the increasing strain on existing fresh water sources, it is apparent that utilizing salt water as a fresh water resource through desalination can become invaluable to solving global water shortages. Currently, the issue is that desalinating ocean water is more expensive than purifying fresh or brackish water resources due to start-up capital and

operational energy costs (Pugsley, Zacharopoulos, Mondol, & Smyth, 2016). By developing lower-energy processes to desalinate ocean water there is potential to create an economical, renewable water supply.

1.1 Desalination Techniques

The leading method of desalination is through reverse osmosis (RO) (Okamoto & Leinhard, 2019). Currently, RO is the most energy-efficient approach but requires several stages of filters to purify water. These filters are not recyclable, so this method leads to large amounts of waste.

The next most common forms of desalination include a variety of distillation methods. Distillation, or phase-change desalination, is not currently as energy-efficient as RO so it is not as common in industrial production water. Improving the energy-efficiency of phase-change desalination could have multiple benefits. First, RO is approaching its theoretical limit of efficiency, while there are many methods of distillation that can be explored that may make it the most energy-efficient method (Elimelech & Phillipl, 2011). Distillation also has the potential to produce less physical waste than popular filtration methods. The materials used in common filtration practices, including RO, are not recyclable and must be disposed of, sometimes even as toxic waste. Distillation has the potential to cut back emissions and reduce waste, which could make it a more sustainable alternative overall when compared to RO. Finally, phase-change desalination can be paired with other manufacturing facilities, such as energy production plants, nuclear reactors, or

other factories that create excess waste heat. In thermal electric power generation facilities, water acts as a coolant for the machinery, and in turn absorbs the energy from the waste heat. If this waste heat can be used for pre-heating a distillation system, this could provide purified water at lower emissions and costs.

1.2 Low Pressure Desalination Potential

To make desalination even more efficient, it could be possible to pair these heat-intensive processes with *low-pressure* systems. This allows the water to vaporize at a lower energy-consumption rate, evaporating the saltwater at lower temperatures to save energy. Vaporization pressure, or the pressure at which a fluid changes phase from liquid to gas, is affected by both the temperature of the fluid and the pressure *around* the fluid. For example, in a high-pressure environment, like a pressure cooker, water will not boil or steam until it is hotter than the typical 212 degrees Fahrenheit (100 degrees Celsius). This allows food to cook faster, since it can be cooked in the higher temperature liquid without the fluid changing phase to steam. In the opposite effect, by *lowering* the pressure of a system, the working fluid (for this study, assumed to be saltwater unless stated otherwise), molecules are able to vaporize more freely. Since salt is a solid, it does not vaporize with the water molecules. Thus, the water vapor can be gathered, condensed, and collected as freshwater.

One of the greatest costs of phase-change desalination is the cost of the energy that it takes to heat the water to sufficient temperatures to vaporize (Pugsley, Zacharopoulos,

Mondol, & Smyth, 2016). Examining the effects of lowering the pressure around the saltwater opens the possibility of creating more energy-efficient, cost-efficient, and overall more sustainable desalination process.

1.3 Significance of the Study

Renewable water production is the leading motivation for this study. The findings will contribute to the industrial and scientific communities and their applications of these principles to large and small-scale desalination.

1.4 Statement of the Problem

Global water shortage has larger implications than an increasingly limited drinking water supply for populations; water is required in agriculture, manufacturing, and in daily household activities, as shown in Figure 3. Currently, the leading method of desalination is through reverse osmosis (RO) (Okamoto & Leinhard, 2019). RO is the most energy-efficient approach but requires several stages of filters to purify water. These filters are not recyclable, so this method leads to large amounts of waste.

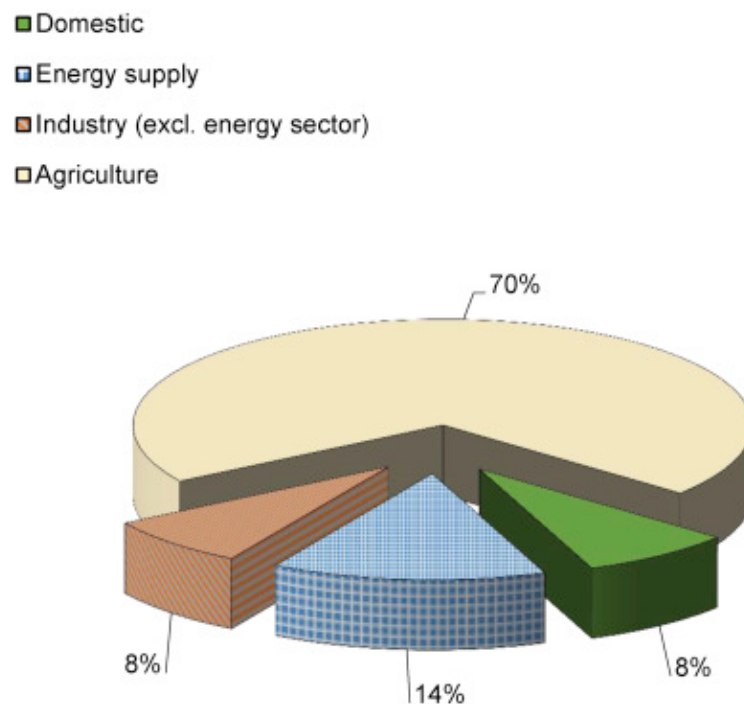


Figure 3: Global use of fresh water based on data from UN-Water (Pugsley, Zacharopoulos, Mondol, & Smyth, 2016).

The benefit to improving the energy-efficiency of phase-change desalination would be both to finding the most energy-efficient means and to produce less physical waste than filtration methods. By cutting back emissions and reducing waste, it can be a more sustainable alternative overall. Finally, phase-change desalination can be paired with other production plants, such as energy plants, nuclear reactors, or factories that create excess waste heat. The water acts as a coolant for the machinery, and in turn is heated by the waste heat. This creates purified water at lower emissions and costs.

To make desalination more efficient, it could be possible to pair these heat-intensive processes with *low-pressure* systems. This allows the water to vaporize at a lower energy-consumption rate and evaporate the saltwater at lower temperatures to save energy. Vaporization pressure, or the pressure at which a fluid changes phase from liquid to gas, is affected by both the temperature of the fluid, and the pressure *around* the fluid. For example, in a high-pressure environment, like a pressure cooker, water will not boil or steam until it is hotter than the typical 212 degrees Fahrenheit (100 degrees Celsius). This allows food to cook faster, since it can be cooked in the higher temperature liquid without the fluid changing phase to steam. In the opposite effect, by *lowering* the pressure of a system, the working fluid molecules vaporize more freely (for this study, assumed to be saltwater unless stated otherwise). Since salt is a solid, it does not vaporize with the water molecules. Thus, the water vapor can be gathered, condensed, and collected as freshwater.

One of the greatest costs of phase-change desalination is the cost of the energy that it takes to heat the water to sufficient temperatures to vaporize (Pugsley, Zacharopoulos, Mondol, & Smyth, 2016). Examining the effects of lowering the pressure around the saltwater opens the possibility of creating more energy-efficient, cost-efficient, and thus more sustainable desalination options.

1.5 Purpose Statement

The purpose of this study is to explore the effect of a low-pressure environment on the mass flow rate of vaporizing water. Past studies conducted on low-pressure boiling and evaporation do not generally share control characteristics, or even describe the same outcomes of their studies (Michaie, Rulliere, & Bonjour, 2019). For example, one study may be seeking information strictly about bubble characteristics under variable conditions without regard for energy efficiency. Another may study heat transfer and energy efficiency, but does not describe the effects of pressure, surface materials or other variables on the results. For this reason, in the developed algorithms, certain assumptions must be made. For example, in the studies done by Michaie, Rulliere, & Bonjour (2019), it was realized that the head height of the heated fluid has a significant impact on heat transfer in low-pressure settings. Until recently, this was not realized by researchers and so not recorded in many studies as a control variable.

Furthermore, the goal of this research is to aid in future applications of seawater desalination. While most studies looked at the effects of boiling water, some used other

working fluids, and very few of them actually studied saltwater (Michaie, Rulliere, & Bonjour, 2019). It is assumed that water and saltwater have very similar properties in terms of mass and heat transfer, so that the equations developed on boiling behaviors can be applied and tested on desalination applications.

The goal of the developed model is to understand how low-pressure *boiling* affect mass transfer. Understanding how mass transfer rates vary under sub atmospheric pressure conditions will help increase system efficiency, aiding the pursuit of sustainable freshwater production.

1.6 Thesis statement

Low pressure distillation has potential to generate a greater fresh water mass, for the same input energy, compared to distillation at STP. A model is developed that relates temperature, pressure, and input heat transfer to the fresh water mass output. The primary result is the ability to estimate fresh water production from low-pressure vaporization.

1.7 Limitations and Assumptions

Brine disposal methods are not specifically explored or discussed in this research. For sustainable, responsible fresh water production, responsible management of the by-product of desalinated waters should be thoroughly explored.

Additionally, the model developed is made with a method known for standard-pressure. The model is purely empirical, however, and should undergo experimental verification.

Though many studies use water as the working fluid in their research, few studies look specifically at saltwater distillation. Until a correlating variable is determined, assume that saltwater follows the same trends as freshwater under variable pressure conditions.

1.8 Thesis Document Organization

This thesis is organized as follows. The scope and diversity of all desalination methods makes it difficult to present a single literature review. Desalination is a broad topic with multiple nuances within sub-categories. For this reason, chapter topics are introduced with a focused literature review in each chapter. Chapter 2 starts with the broadest methods of desalination. Chapters 3 and 4 focus on Reverse Osmosis and Vacuum Distillation, respectively. Chapter 5 presents conventional boiling mass transfer models at standard temperature and extends these to low pressure. Chapter 6 concludes the document with a summary of the conclusions and suggestions for future work.

1.9 Definitions of Terms

Boiling Boiling is classified as “pool boiling” or “flow boiling” (Cengel & Ghajar, 2016)

Brine The salty discharge produced during the desalination process.

Cavitation	When the pressure within a fluid becomes “low enough to cause water to [vaporize] generating vapor bubbles which, when reaching regions of higher pressure, will implode releasing energy” (Rosa, 2013).
Diffusion	The movement of a species in a solution from an area of high concentration to an area of low concentration (Feher, 2017).
Evaporation	The occurrence of phase change from liquid to vapor at the “liquid-vapor interface when the vapor pressure is less than the saturation pressure of the liquid at a given temperature” (Cengel & Ghajar, 2016).
Flow boiling	Fluid “is forced to move in a heated pipe or over a surface by external means such as a pump. Therefore, flow boiling is always accompanied by other convection effects” (Cengel & Ghajar, 2016).
Permeate	The freshwater product produced during reverse osmosis.
Pool boiling	“In pool boiling, the fluid body is stationary, and any motion of the fluid is due to natural convection currents and the motion of the bubbles under the influence of buoyancy... Pool boiling of a fluid can also be achieved by placing a heating coil in the fluid” (Cengel & Ghajar, 2016).

Reverse Osmosis	Seawater “is pressurized against a semi-permeable membrane that lets water pass through but retains salt... At present, reverse osmosis is the most energy-efficient technology for sea-water desalination” (Elimelech & Phillipl, 2011).
Saturated boiling	Also known as <i>bulk</i> boiling; “when the temperature of the liquid is equal to the saturation temperature” (Cengel & Ghajar, 2016).
Subcooled boiling	“When the temperature of the main body of the liquid is below the saturation temperature” (Cengel & Ghajar, 2016).
Subcooling degree	Difference in temperature between the bulk of the fluid and the fluid at the surface of the heat source (Del Valle M & Kenning, 1985).
Thermophoresis	“Thermophoresis is a force generated by the temperature gradient between the hot gas and the cold wall effecting the particulate movement towards the cold wall” (Glensvig, Stowe, & Schutting, 2013).

1.10 List of Acronyms

MED	Multiple Effect Distillation
MSF	Multi-Stage Flash
NREL	National Renewable Energy Laboratory
RO	Reverse Osmosis

VC	Vapor Compression
WWAP	World Water Assessment Programme
STP	Standard Temperature and Pressure

2 Methods of Desalination

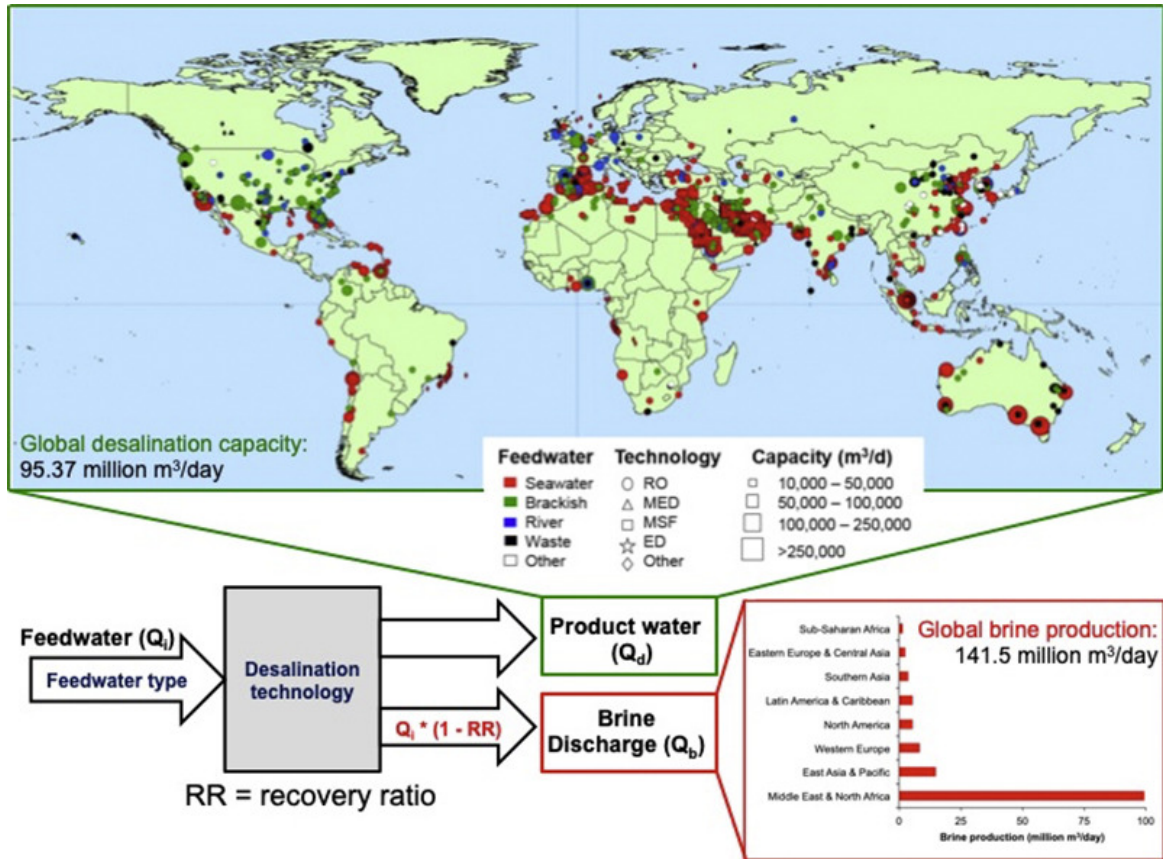


Figure 4: Graphical display of volume of water produced across the globe (Jones, Qadir, van Vliet, Smakhtin, & Kang, 2019).

Currently, it is estimated that about 15,900 desalination plants produce around 95 million m³/day of fresh water around the world (Jones, Qadir, van Vliet, Smakhtin, & Kang, 2019). As seen in Figure 4, coastal cities are the most prone to utilizing nearby salt water as an opportunity to decrease water stress through desalination.

A multitude of desalination methods are currently utilized. Described below are several of the most common methods, in addition to ideas mentioned in studies that have not yet been applied industrially.

2.1 Desalination Methods

The taxonomy in Figure 5 shows the methods of desalination discussed throughout this paper.

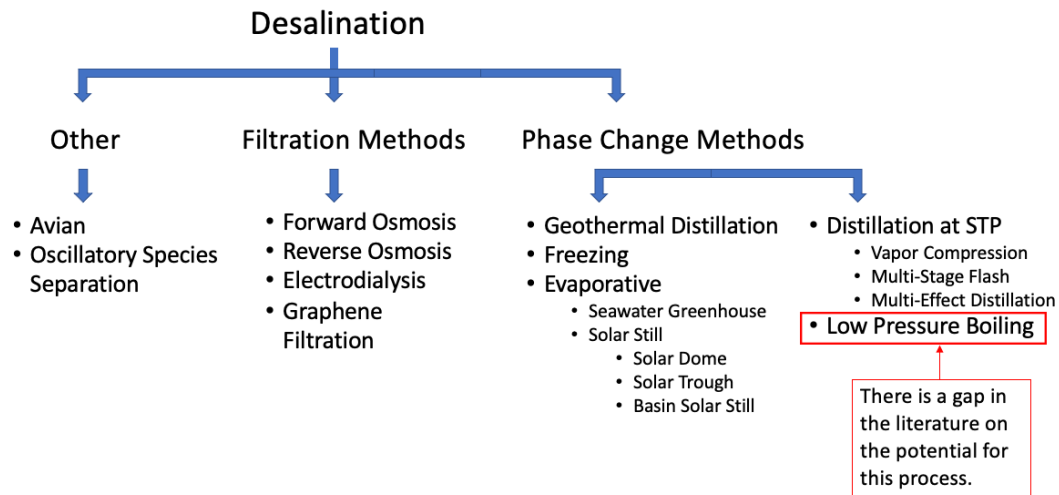


Figure 5: Taxonomy of the methods of desalination outlined in this paper.

2.2 Biological Filtration - Avian

Though not a mechanical system, desalination happens in nature every day through biological filtration, illustrated here specifically by avian filtration. This is simply the biological process that birds living in saltwater environments employ to properly hydrate

through the consumption of saltwater. As is commonly known, if a human drinks seawater, they will not be hydrated, but will instead actually accelerate the dehydration process due to the salt content of the water. There are many breeds of marine birds, however, that not only drink salt water, but also consume foods such as crab that have an even higher salt content, without getting overly dehydrated.

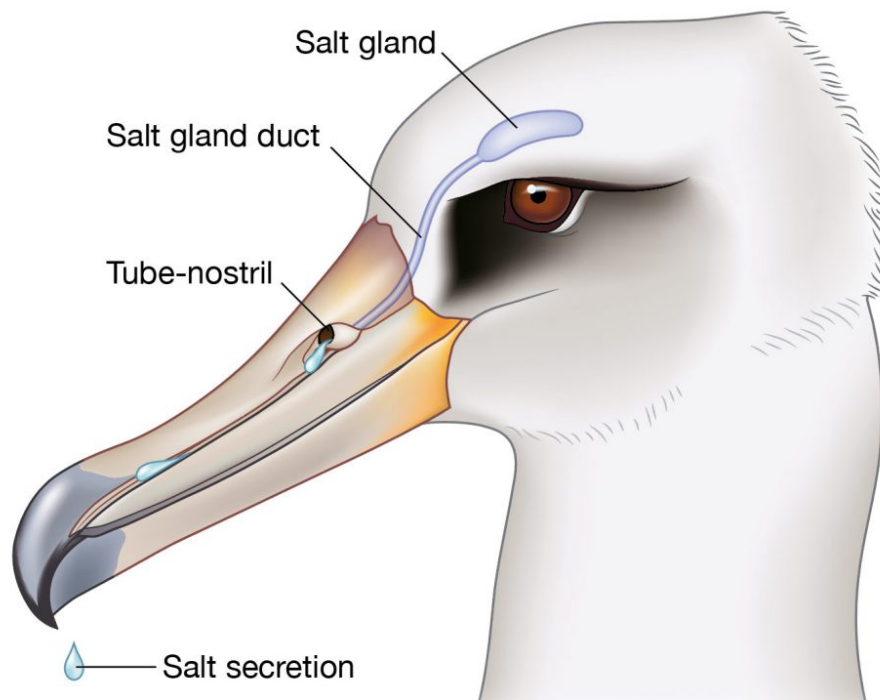


Figure 6: Image of the salt removal mechanism in marine birds (Lovette & Fitzpatrick, 2017).

As seen in Figure 6, marine birds are born with salt glands and ducts within their bills that rid the body of excess salt (Lovette & Fitzpatrick, 2017). In a study conducted by physiologist Knut Schmidt-Nielsen, a gull ingested about 10 percent of its body mass in

seawater and after three hours the bird had “totally eliminated the salt load, mostly via excretions from its salt glands” (Lovette & Fitzpatrick, 2017). In addition to the salt glands, the kidneys in these types of birds help to filter out any remaining salt that is ingested. In contrast to a marine bird, if a human of about 150 pounds drank 2 gallons of saltwater, or about 10 percent of their mass, it would be more than a lethal amount according to Schmidt-Nielsen.

This method of “desalination” is not immediately helpful as an engineer designing a mechanical purification system. Regardless, approaching the problem-solving process as open-minded as possible has led to some of the best innovations in human history. Perhaps, upon further investigation, avian desalination will unlock some key methods to human water security in the future.

2.3 Oscillatory Species Separation

Research conducted through several partnerships at the University of Florida investigates the potential of “oscillatory flow as a means of enhanced species separation” (Crain, Oropeza, Divo, Kassab, & Narayanan, 2006). The researchers concluded that a species separation device could be created utilizing oscillatory flow. This means that the separation is purely a mechanical action when the correct oscillation pulse rates are set. This numerical research could someday have implications in desalination as well.

Recent research in desalination does not specifically talk about oscillatory flow as a means of purification. However, membrane oscillation has been investigated to find out

if membrane fouling can be reduced. Membrane fouling is an issue because the accumulation of particulates on purification membranes decreases permeate flux, and also increases the pressure drop across the membrane (Ullah, Shahzada, Khan, & Starov, 2020). Typically, in cross-flow membranes this fouling is minimized by using layer separations within the membrane that will create turbulence within the fluid to help lift away deposited particulates. Ullah et al. investigate the possibility of oscillating the entire membrane unit to break the particulates free of the membrane surface.

The goal of the membrane oscillation research is very different than the research conducted by Crain et al. It is possible that the research on oscillatory flow separation could be applied in desalination as a method that does not need membranes or added heat. It is unclear how energy-efficient this would be compared to current methods. Further research within desalination specifically would need to be investigated.

2.4 Graphene Filtration

Graphene is a material made of carbon atoms bonded together in hexagonal patterns (Boretti, et al., 2018). Graphene was first discovered in 1962 and rediscovered in 2004 by Novoselov and Geim (Boretti, et al., 2018). Graphene has had an increasing level of interest in several applications, including desalination. It is a one-atom thick material and so is considered to be 2D as is illustrated in Figure 7. Because of this, many scientists are exploring its applications as a high-efficiency filtration membrane in desalination (Boretti,

et al., 2018). It is believed that it could be used as the membrane material in ultrafiltration, forward osmosis, or reverse osmosis applications.

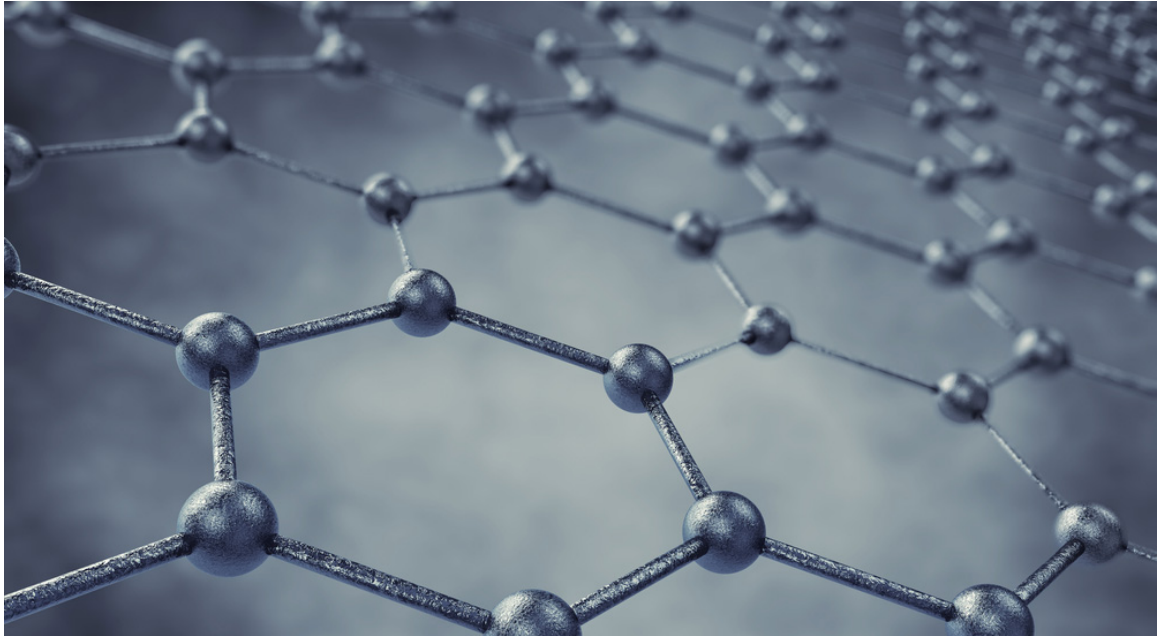


Figure 7: Representation of the 2D material, graphene (Boretti, et al., 2018).

As of 2018, the development of mass-production technologies for graphene was just getting off the ground in laboratories at MIT (Chu, 2018). Because of current production limitations, graphene has not yet been used in industrial applications.

2.5 Electrodialysis

Electrodialysis (ED) desalination and a similar method known as electrodialysis reversal (EDR) “use electrical current to move ions selectively through membranes that are embedded with ion exchange resins, leaving purer water behind” (Veerapaneni, Long, Freeman, & Bond, 2007). According to Veerapaneni et al., the energy consumption of ED

or EDR to remove the ionic material contained in high salinity seawater is not viable compared to other methods of desalination. For this reason, it is a purification method that may have applications in brackish water, but the authors recommend a thorough life cycle and cost analysis before implementation (Veerapaneni, Long, Freeman, & Bond, 2007). The reason for this is that the higher the salt content, the more energy it takes to remove the ions, or the salt molecules. Brackish water is a mixture of fresh and saltwater, typically found in estuaries or in some cases wells that are close to the shoreline. In these cases, ED and EDR offer competitive energy savings, but for seawater desalination the technology is not sufficient.

2.6 Geothermal Desalination

Geothermal energy is a renewable resource that has been explored by humans for a very long time. Something as simple as using hot water from geysers to cook food, as is a tradition by the Moaris people in New Zealand, is a method of utilizing geothermal energy (Newton, 2011). Earth's core is projected to produce temperatures as high as 8,000 degrees Fahrenheit. Heat is also generated in the mantle and crust due to the radioactive decay of certain elements, such as uranium (Newton, 2011).

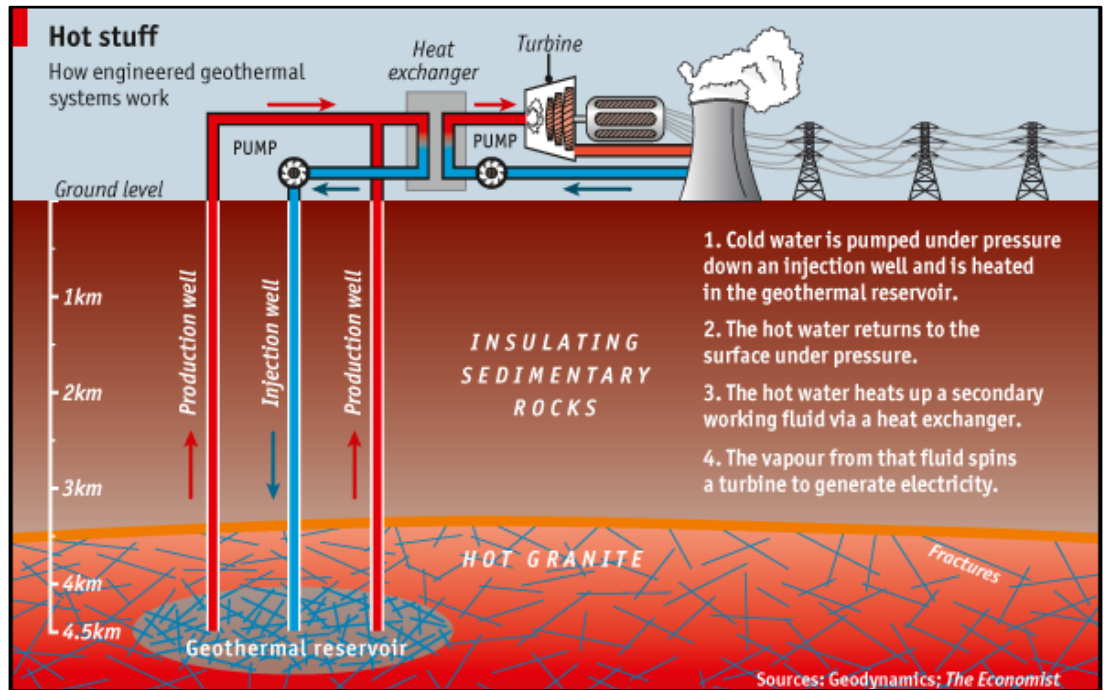


Figure 8: Geothermal system utilized for energy production (REVE, 2013).

Geothermal energy utilizes this essentially infinite heat resource from the earth to generate energy. Generally, hot steam or super-heated water is pumped from these hot areas to the earth's surface, where the vapor can be used to turn a turbine and generate electricity. This energy resource could be a great aid to producing fresh water through desalination. In regions with geothermal energy available near a seawater resource, such as Djibouti or Saudi Arabia, seawater can be heated using the geothermal heat (Chandrasekharam, Lashin, Arifi, Al-Bassam, & Varun, 2019; Chandrasekharam, D., Lashin, Arifi, Al Bassam, & Varun , 2017). This would greatly reduce or eliminate the need for carbon emissions in a distillation method of desalination.

Geothermal desalination does have limitations, however. It is important that geothermal sites are not located too closely to other sites, and seismic activity for a region should be considered before a geothermal well is installed (Zaal, Daniilidis, & Vossepoel, 2021). It is also expensive to install a geothermal site, so it is important to conduct a thorough economic analysis to ensure that enough heat can be produced from the site to offset costs (Zaal, Daniilidis, & Vossepoel, 2021).

2.7 Freezing Desalination

Through analysis of polar ice caps, it is apparent that salt water can freeze, and as it freezes, it is no longer salty. Using this natural phenomenon as inspiration, freezing desalination is a potential method of fresh water production. Biomimicry, or “design by analogy to biology... is innovation through the emulation of biological forms, processes, patterns, and systems” (Kennedy, 2017). Exploring natural processes can be an excellent path to more environmentally friendly designs across engineering, including in desalination.

The freezing desalination process is straightforward. When seawater freezes, the ice contains very little salt because only the water molecules freeze (NOAA (National Oceanic and Atmospheric Administration), 2004). The process then consists of three steps which imitate this natural ice forming process: ice formation, ice cleaning, and melting the ice.

To follow this process artificially, salt water is first passed through a heat exchanger. This reduces the temperature of the water until it is near (but not at) its freezing point.

Then, the chilled seawater is placed into a freezer to form it into ice. As the water freezes, the salt is extruded as the water molecules freeze but the salt ions do not. This forms a salty brine around the exterior of the ice. Before warming the ice back up to melt it into fresh water, this brine layer must be washed away.

It is estimated that the energy consumption of freezing desalination could provide an energy savings of 75-90% when compared to other thermal distillation or evaporative processes since the heat of fusion of ice is 333kJ/kg, compared to 2,500kJ/kg heat of vaporization (El Kadi & Janajreh, 2017). A major drawback to freezing desalination is that it must be done in batch processes. Unlike other methods of desalination, water production could not be easily scaled up or down to meet municipality needs. Ice can only freeze and melt so fast, so if the water demands exceeded this pace, it could create supply issues.

2.8 Seawater Greenhouse

In another form of a biomimicry design, seawater greenhouses mimic the natural hydrological cycle of the biosphere (Yeang & Pawlyn, 2009). Cardboard “grilles” at the front of the greenhouse evaporate seawater to create cool humid air, which is then condensed as distilled, fresh water at the back of the greenhouse. Various versions have already been implemented in Tenerife, Oman, and the United Arab Emirates (Yeang & Pawlyn, 2009). Figure 9 below shows a typical seawater greenhouse setup.

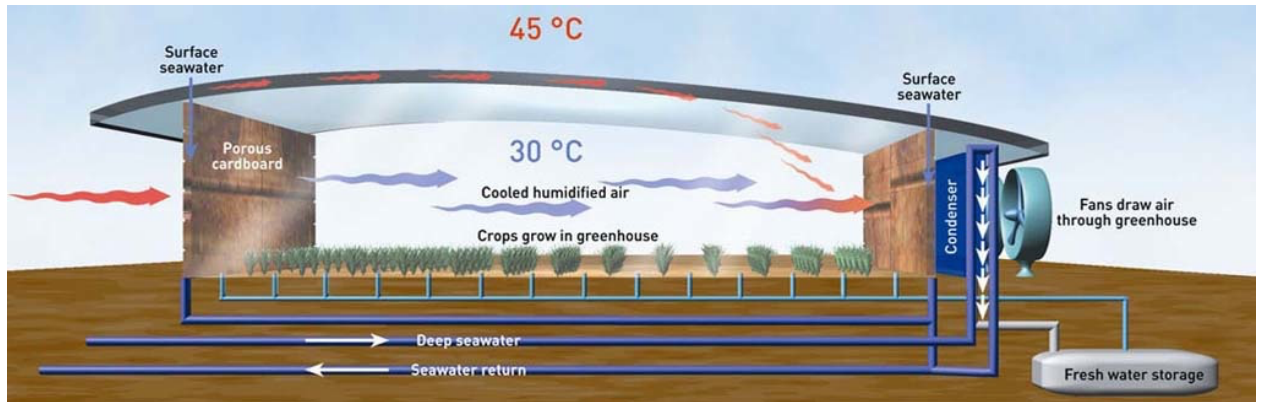


Figure 9: Schematic of a seawater greenhouse setup for an arid climate (Cho, 2011).

This technology is already being tested and applied. In the Desert of Jordan, King Abdullah II of Jordan and the Crown Prince Haakon of Norway created a partnership in 2017 that has led to a sustainable farming initiative (Borgen, 2019). The project seeks to utilize solar energy and salt water as the main inputs in an initiative to create fresh water, food, and sustainable jobs in this desert region. In Figure 10 below, the layout of the facilities is shown. The plan is to incorporate seawater greenhouses, an algae facility, external vegetation and evaporative hedges, research facilities, evaporative ponds and concentrated solar power facilities (Sahara Forest Project, n.d.)

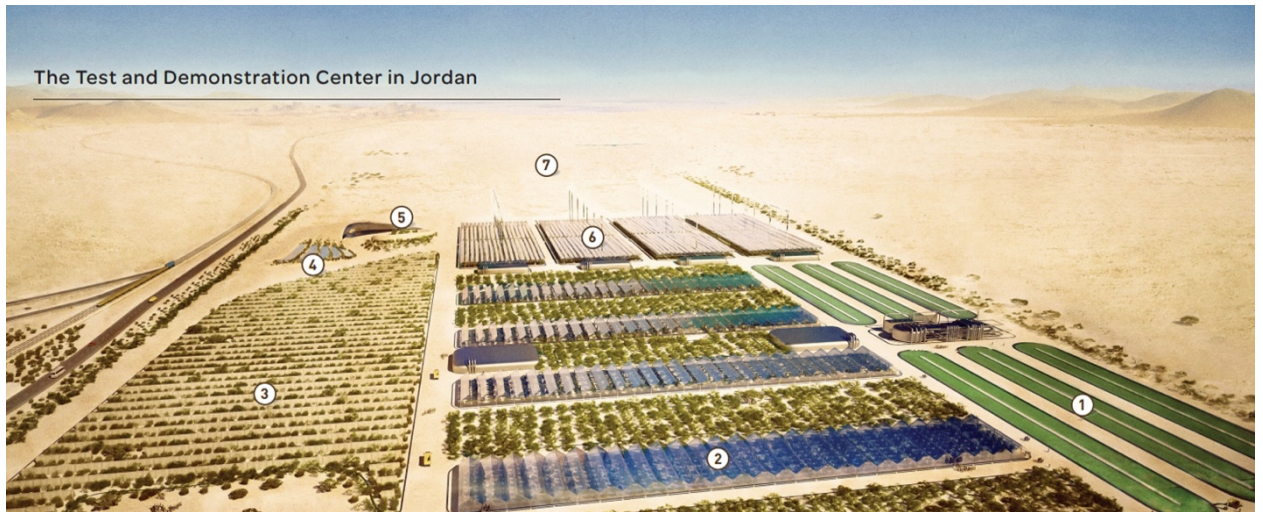


Figure 10: The test and demonstration center for the seawater greenhouse setup in Jordan (Sahara Forest Project, n.d.).

A seawater greenhouse is best implemented in dry, arid environments. Dry air encourages the evaporative process. The saturated cardboard grilles help to humidify the air within the greenhouse through evaporation and diffusion, which is the tendency of a species to migrate from a highly concentrated region to a lower-concentrated area (Feher, 2017). If this method were to be implemented in a highly humid region, such as Florida, for example, the evaporative process would be hindered by the amount of natural moisture in the air, even if there is an abundance of sunlight.

2.9 Solar Still

A solar still is defined here as any method of distillation utilizing solar thermal energy to increase evaporative desalination. The salt within the seawater does not

evaporate, so as the water heats up, water molecules break from the surface as water vapor. Then, typically in a solar still, there is a method of capturing the recondensed water.

In Figure 11 and Figure 12 below, there is a hollow, plastic, buoyed dome that floats on the surface of the sea. Incident light from the sun heats the interior of the buoy and causes the water to evaporate. The water condenses across the top of the dome, drips down the sides, and is collected as fresh water.

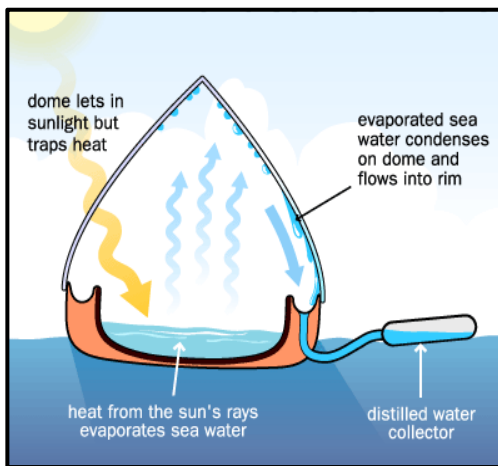


Figure 11: Schematic of solar dome (How Solar Stills Work, 2012).

Figure 12: Image of a solar dome (How Solar Stills Work, 2012).

There are other designs for solar stills, as well. In a tubular solar still, saline water in a flat plate is processed within a larger tube. Similar to the buoy system, as the water evaporates, it condenses on the top of the tube and is collected at the bottom, as shown in Figure 13 and in Figure 14 below.

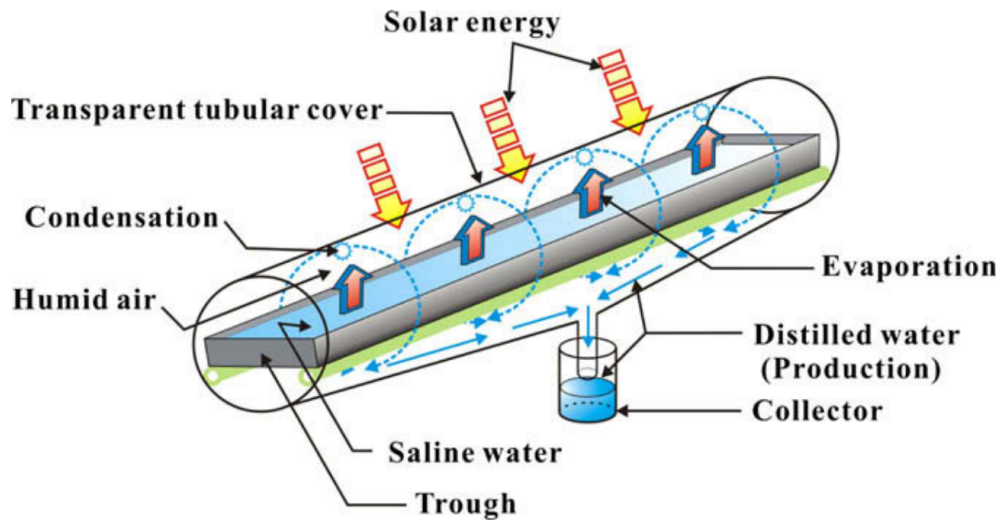


Figure 13: Overview of a solar trough (Ahsan & Fukuhara, 2010).

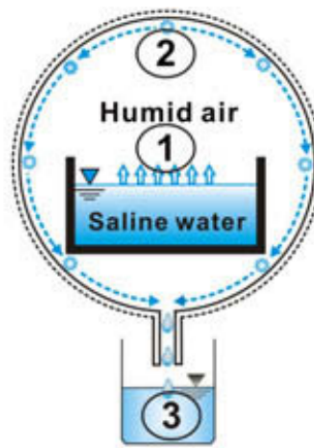


Figure 14: Side view of a solar trough setup (Ahsan & Fukuhara, 2010).

Another common form of the solar still is the “basin-type” (Ahsan & Fukuhara, 2010). Here, large rectangular basins made of clear material have a thin layer of salt water at the bottom. As with the previous two designs, the condensate gathers on the roof and is

collected. In these, it is typical to have a slanted roof for two purposes; first, the water has an easy, downward path to follow to condensate collection. Secondly, the tilt is usually angled intentionally towards the sun in order to collect more heat through sunlight. The process for a standard, basin-type still is shown in Figure 15 below.

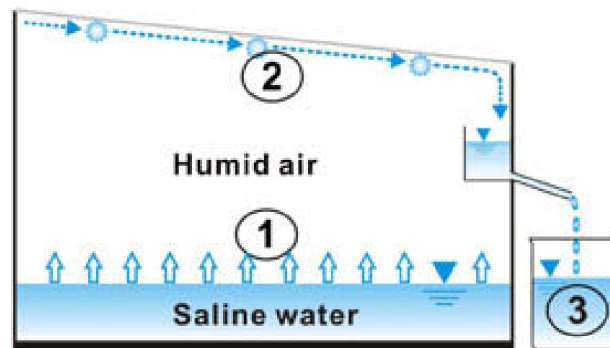


Figure 15: Basic form of a basin-type solar still (Ahsan & Fukuhara, 2010).

In these conventional stills where solar radiation is transmitted through the top clear cover, the average production rate is 1-2L/m²/day (Patel, Markam, & Maiti, 2019).

2.10 Distillation at STP

Distillation desalination includes any method that involves boiling saltwater in order to create fresh water vapor. Several of the methods of desalination currently in practice pair desalination plants with power plants to utilize waste energy to heat the saltwater, while using the saltwater as a coolant for the power plant (Pugsley, Zacharopoulos, Mondol, & Smyth, 2016). Another potential source of heat for the saltwater could be solar thermal

energy, or utilizing the natural energy provided through solar radiation. This is demonstrated in Figure 16. For any method of distillation, the heat necessary to get the water to the boiling point places high energy requirements on the system (Pugsley, Zacharopoulos, Mondol, & Smyth, 2016).

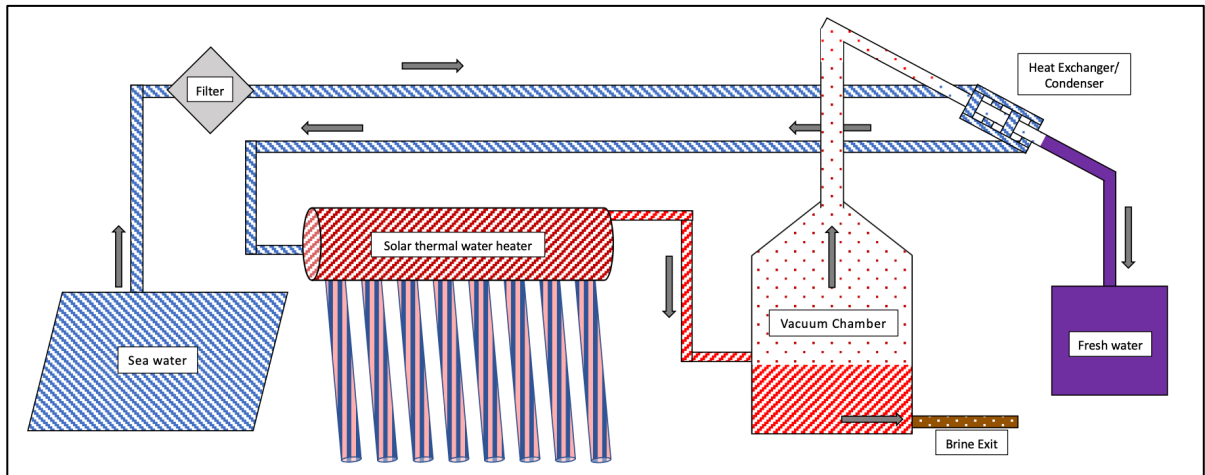


Figure 16: Schematic of an example of the system setup that inspired this study.

If water can be vaporized in a low-pressure system, there is potential to decrease the necessary minimum boiling temperature, greatly saving energy requirements. Water vaporization pressure is defined as the pressure at which water molecules release from the liquid mass as gas molecules (Michaie, Rulliere, & Bonjour, 2019). It is easier for water molecules to change phase into gas molecules at lower pressures. This means that less heat must be added to achieve phase change which can significantly reduce the energy necessary to vaporize water. Figure 17 illustrates the relationship between phase change, pressure,

and temperature to show the benefit of lowering the pressure on decreasing the necessary heat or energy.

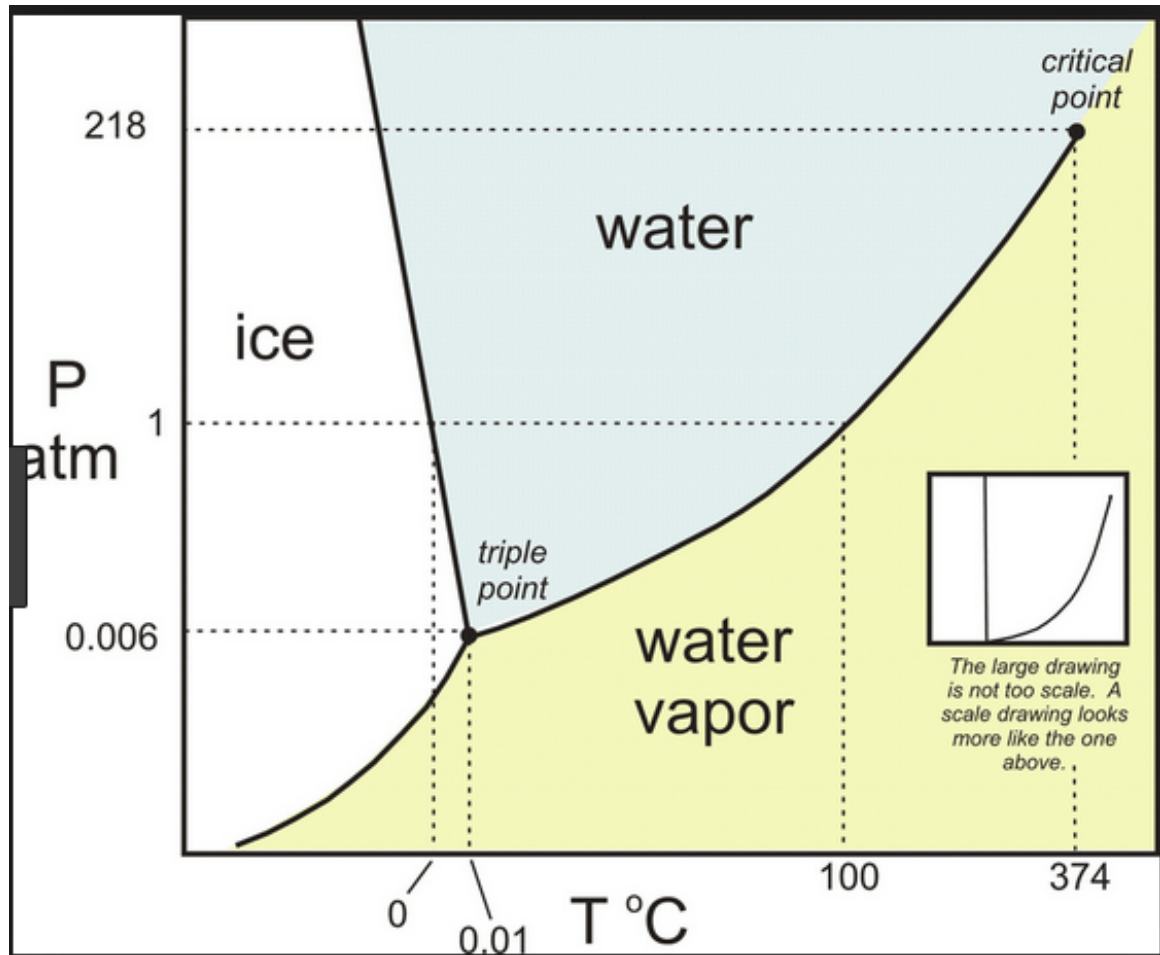


Figure 17: The figure above shows the relationship between temperature and pressure regarding the phase change of water.

The goal of vaporization via distillation is that the salt is left behind while all the molecules that vaporize are pure water. The fresh water is initially in the form of steam, or vapor. Then, through a cooling method dependent on the system design, the vapor is

condensed and collected. The brine, or concentrated saltwater, is disposed of while the collected freshwater can be distributed (Al-Karaghoul, Kazmerski, & (NREL), 2013).

There are multiple methods of seawater distillation in industrial desalination. The most used examples include multi-stage flash (MSF), multi-effect distillation (MED), and mechanical vapor compression (MVC) distillation.

2.10.1 Multi-Stage Flash Distillation

MSF utilizes thermal and electrical energy to send saltwater through a series of stages, with each stage successively lowering in both temperature and pressure. The lower pressure in each stage causes the water to “flash evaporate” or steam rapidly from the brine. The steam is collected and used as heat in the other stages, and as a function of the heat exchange process, is cooled and condensed, then collected as freshwater (Al-Karaghoul, Kazmerski, & (NREL), 2013). An example of an MSF unit is shown in Figure 18.

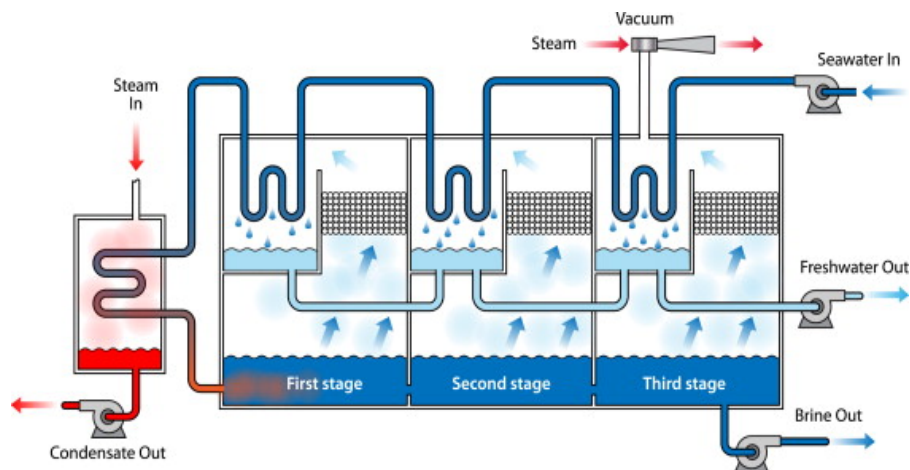


Figure 18: Schematic of MSF unit (Al-Karaghoul, Kazmerski, & (NREL), 2013).

The first stage has the highest pressure because it is operating at the highest temperature, thus creating the most steam. The steam production affects the stage pressure. The less-hot water in the second stage produces less steam, also producing less pressure in the system. This continuous cycle of equilibrium-driven vaporization in each cycle produces a maximum amount of fresh water vapor without having to add heat at every stage.

2.10.2 Multi-Effect Distillation

MED is similar to MSF in that it often utilizes waste heat from other industrial processes, incorporates variable pressures and temperatures, and has a series of stages to desalinate water. In MED however, saline water is sprayed across heated tubes. Some of the water vaporizes on contact with the tubes, while the concentrate falls into the bottom of the container as brine. The vaporized water is collected and used in the heated tubes of the next phase (Al-Karaghoul, Kazmerski, & (NREL), 2013). Figure 19 shows an example of an MED unit.

Also like MSF, each stage is driven by vaporization pressure equilibrium and allows for only one point of heat addition with multiple stages of vaporization at multiple temperatures and pressures.

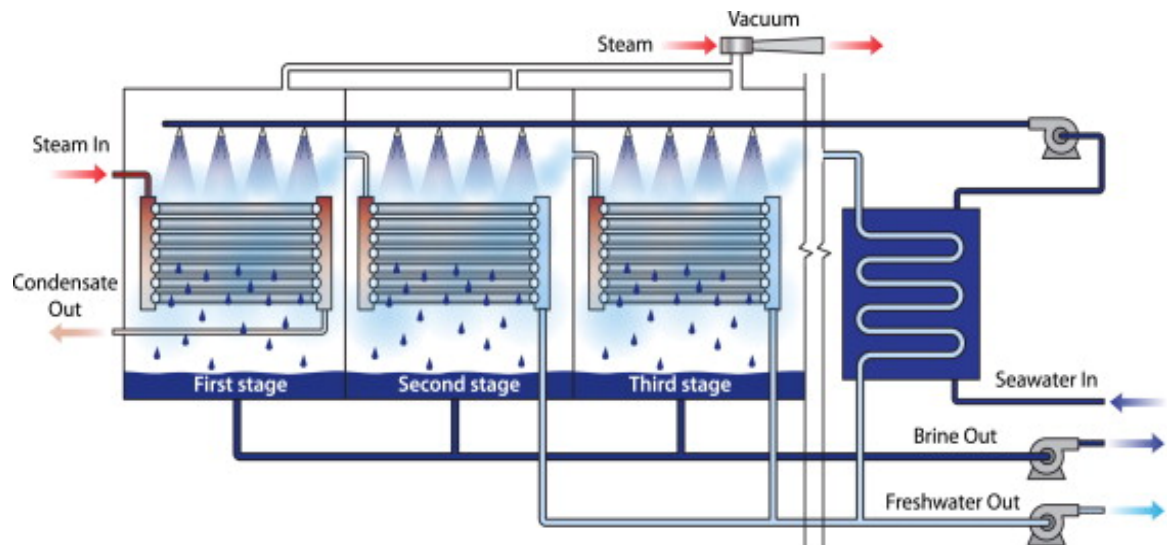


Figure 19: MED unit setup (Al-Karaghoul, Kazmerski, & (NREL), 2013).

2.10.3 Mechanical Vapor Compression

MVC distillation follows the same principles as MED, but the collected freshwater steam is compressed in a vapor compressor before being fed through the heat exchanging tubes so that the steam is hotter. Also, MVC is usually only a one-phase process, instead of sending the water through multiple stages as is typical in MED and MSF, as shown in Figure 20 (Al-Karaghoul, Kazmerski, & (NREL), 2013).

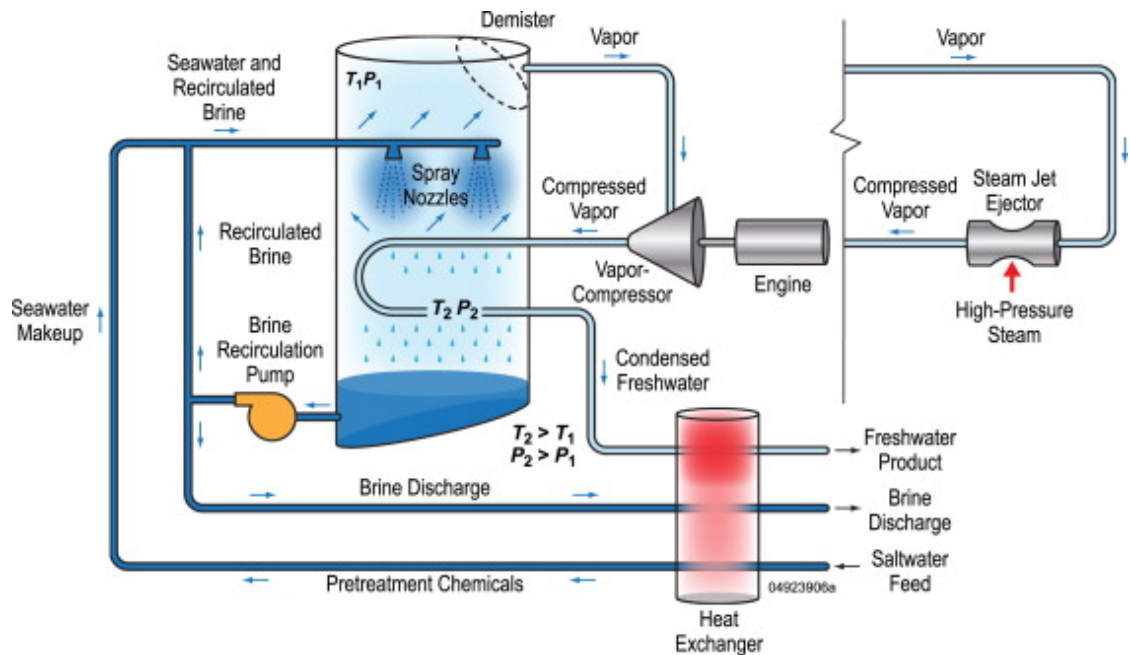


Figure 20: Schematic of a vapor compression unit (Al-Karaghoul, Kazmerski, & (NREL), 2013).

2.11 Reverse Osmosis

During reverse osmosis, sea water “is pressurized against a semi-permeable membrane that lets water pass through but retains salt” (Elimelech & Phillipl, 2011). It is currently the leading method of desalination globally, in addition to being the most energy-efficient method.

There are several pros to reverse osmosis. As mentioned, it is the most energy efficient. Additionally, it is relatively simple to scale a reverse osmosis system up to meet production needs. An adverse side of reverse osmosis is that the membranes are expensive to create and have a cradle-to-grave lifecycle, meaning that once a membrane is out of service it goes to a landfill. There is not yet a way to recycle or reuse membrane materials. Because reverse osmosis is such a prominent method of desalination, it is explored in further detail in Chapter III.

2.12 Conclusion

The methods listed in this chapter range from purely theoretical to fully functional and utilized at massive municipal scale. To summarize, each method is listed in the table below, along with their average energy intensity (if it is known), and the author’s assessment of their technology readiness level (TRL).

TRL’s were originally developed by NASA in the 1970’s for space technology (TWI, 2021). Shown below is the widely accepted scale for TRL.

TECHNOLOGY READINESS LEVEL (TRL)

RESEARCH	9	ACTUAL SYSTEM PROVEN IN OPERATIONAL ENVIRONMENT
	8	SYSTEM COMPLETE AND QUALIFIED
	7	SYSTEM PROTOTYPE DEMONSTRATION IN OPERATIONAL ENVIRONMENT
DEVELOPMENT	6	TECHNOLOGY DEMONSTRATED IN RELEVANT ENVIRONMENT
	5	TECHNOLOGY VALIDATED IN RELEVANT ENVIRONMENT
	4	TECHNOLOGY VALIDATED IN LAB
	3	EXPERIMENTAL PROOF OF CONCEPT
RESEARCH	2	TECHNOLOGY CONCEPT FORMULATED
	1	BASIC PRINCIPLES OBSERVED

Figure 21: Widely accepted stages for TRL (TWI, 2021).

Table 1 below gives the energy intensity (if known), the author’s assessment of the TRL of the technology and a brief summary of why that TRL was assigned.

Table 1.1: Summary of desalination methods in both energy consumption, TRL and applicability (Al-Karaghoul, Kazmerski, & (NREL), 2013).

Method	Energy Intensity (kW h/m³)	TRL	
Graphene Filtration	NA	3	Graphene has been developed in laboratory settings but has yet to be utilized in any desalination experiments.
Electro-dialysis (ED)	2.64-5.5	9	Works best with low-saline water but can be used for sea water.
Freezing desalination	NA	8	Municipal freezing systems have been built and used but are uncommon today.
Avian Filtration	NA	1	Not an effective method for small or large scale fresh water production.
Geothermal Desal.	NA	9	Geothermal desalination plants are operational and functioning, but the application is limited based on geothermal energy availability and economic feasibility.

Seawater Greenhouse	NA	9	Seawater greenhouses are in use globally but are limited in their usefulness by region and environmental conditions.
Oscillatory Species Separation	NA	1	This theory has not been applied directly to desalination. There is potential for an effective method of desalination here, but it requires further research and development.
Solar still	0*	9	Effective for small output needs especially in regions that may not have reliable access to electricity. *Requires no electrical energy input as these are always purely thermal systems.
Multi-Stage Flash (MSF)	19.58-27.25	9	Effective for various levels of salinity. Pairs well with plants that produce high levels of heat.
Multi-Effect Distillation (MED)	14.45-21.35	9	Effective for various levels of salinity. Pairs well with plants that produce high levels of heat.

Mechanical Vapor Compression (MVC)	7-12	9	Effective for various levels of salinity. Pairs well with plants that produce high levels of heat.
Seawater RO (SWRO)	4-6	9	Utilized globally, can be scaled up easily.
Brackish Water RO (BWRO)	1.5-2.5	9	Energy savings compared to SWRO come from the decreased number of salts and total dissolved solids (TDS) within the input water.

3 Reverse Osmosis

3.1 History of Reverse Osmosis

Exploration into desalination techniques became very popular after World War II. Techniques that had been used on rafts and ships throughout the war were becoming of greater interest to civilian populations, particularly in California where they were experiencing drought (Aultman, 1949). At the time, distillation was the primary method used, and though it was efficient enough for the relatively small amounts needed aboard ships, scaling the systems to larger outputs was so costly that it did not make economic sense to use the same applications at municipal scale.

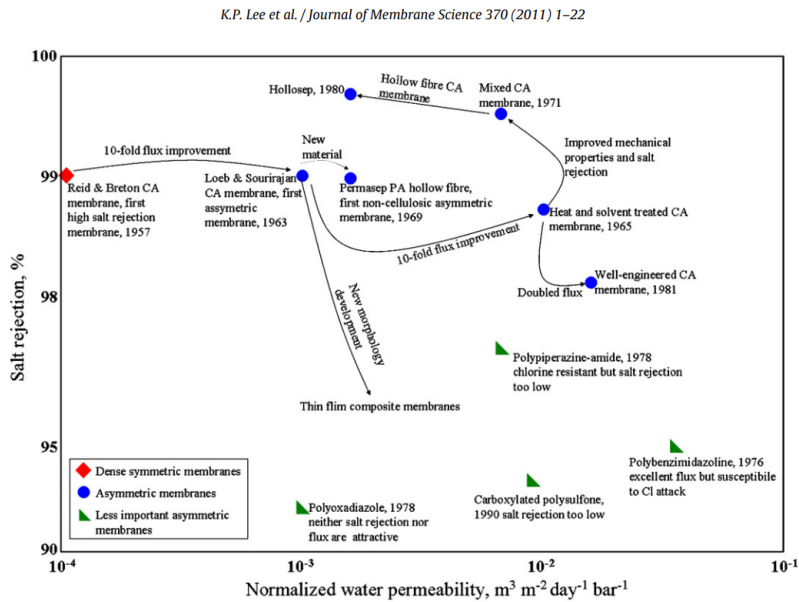


Figure 22: Development of asymmetric RO membranes (Lee, Arnot, & Mattia, 2010).

Exploration of the use of pressurized systems to force water through porous materials began as early as just before the turn of the 20th century, though high yields of freshwater were not produced. Even through breakthroughs in the 1950's where up to 98% salt rejection could be achieved with cellulose acetate membranes, they "provided such small product water volumes that flux levels were reported in units of $\mu\text{L}/\text{cm}^2\text{h}$ " (Glater, 1998). A breakthrough in the late 1950's on asymmetric membranes finally brought researchers to the conclusion that membrane filtration could become economically feasible, and the first commercial desalination plant was installed in Coalinga, California. This facility provided 5,000 gallons per day of drinking water to the community (Glater, 1998). By the mid 1960's, Dow Chemical and DuPont had invested heavily in membrane research and development and were able to bring the products to market on large scales for desalination. The technology of membrane production has not varied hugely since, though more breakthroughs on prefiltration practices, energy recovery techniques, and methods of avoiding membrane fouling have allowed for reductions in cost and energy consumption over the past several decades. Since the 1970's, energy consumption has decreased from 12kWh m^{-3} to less than 2kWh m^{-3} in 2006 for freshwater production utilizing reverse osmosis (Lee, Arnot, & Mattia, 2010).

3.2 How RO Works

3.2.1 System Level Structure

Depending on the desired output flow rate, RO systems have different set-ups, but the overall process is similar across systems. Most require a feed pump to get the original, untreated water through prefilters. From there, a booster pump will get the water up to the pressure needed to overcome the osmotic pressure. Osmotic pressure is required to separate the water molecules from the other molecules in the water, such as salt, bacteria, or other factors of turbidity. The schematic below shows an example of the setup of a reverse osmosis system.

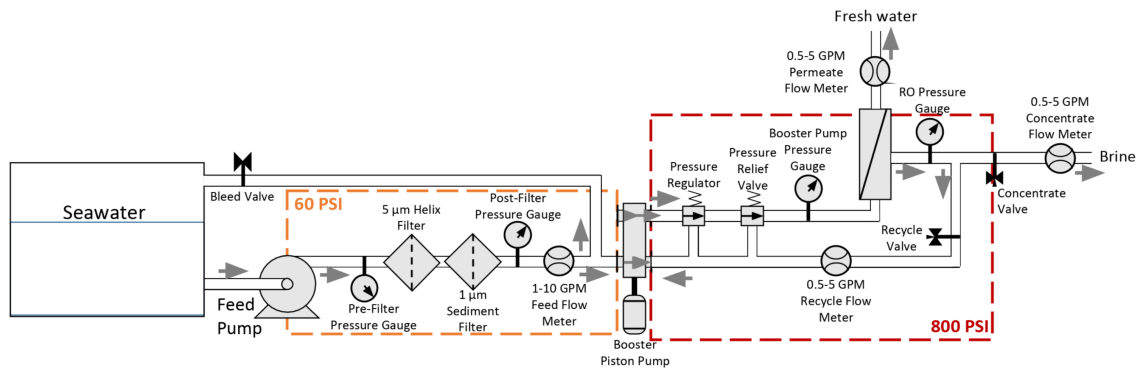


Figure 23: Shown above is the setup for the reverse osmosis unit in the Energy Systems Laboratory at ERAU.

Other symbols shown above include check valves, pressure gauges, and flow meters. These all contribute to the efficiency and usability of the system.

In large systems, it is possible to attach RO membranes either in series or in parallel to improve performance and permeate output. In reverse osmosis systems, the output fresh water is referred to as “permeate.” A very positive aspect of RO desalination is the easy ability to scale systems up based on need. The Tampa Bay Desalination plant in Tampa, Florida is the largest desalination plant in the United States and produces anywhere from 10-15 million gallons per day (Cohen, Semiat, & Rahardianto, 2017). To contrast this, the single membrane unit on Embry-Riddle’s campus produces about a gallon a minute in optimal conditions, which would max out at about 1,400 gallons per day.

3.2.2 Membrane Level Structure

The most common RO membranes in use today are spiral-wound composite membranes. These have a porous plastic tube running through the middle of the membrane. Attached to this are several layers of membrane, feed spacers, and permeate collection layers. The feed water is forced into the layers at a high pressure. The high pressures force the water inward, so that only freshwater makes its way out of the permeate tube.

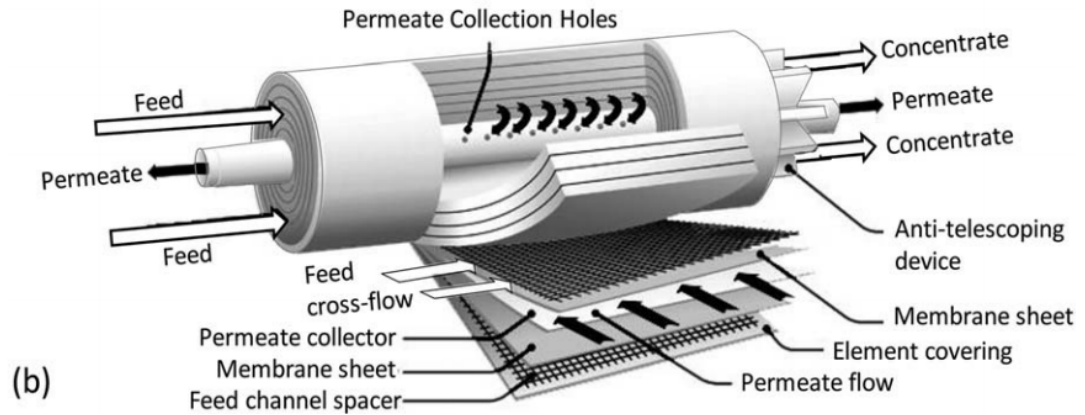


Figure 24: Structure of a typical spiral-wound membrane (A Perspective on Reverse Osmosis Water Desalination: Quest for Sustainability).

Most membranes today are made of thin film composite (TFC) polyamide membranes. They have high water permeability, high salt rejection, and a higher tolerance to a range of temperatures and pH levels (Okamoto Y. , 2019). There are other types of membranes as well, depending on the needs of the consumer and the preference of the manufacturer.

The membranes are created by chemically treating one side of flat sheet. It is the only way to achieve pore sizes small enough to get to the scale of RO filtration. Below is a diagram comparing RO exclusion sizes with common constituents within water.

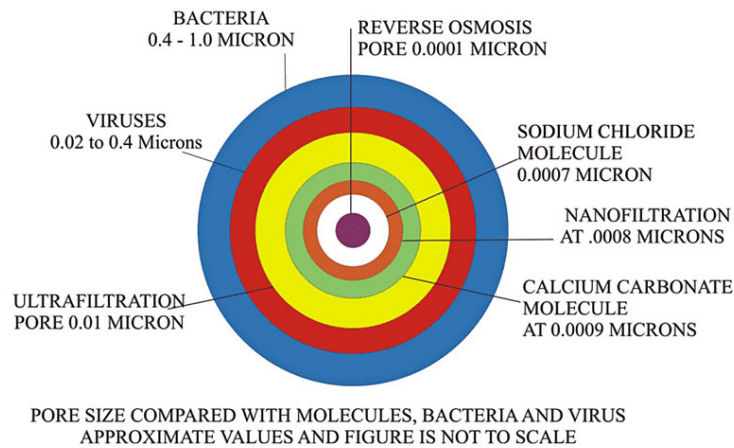


Figure 25: Shows the size of RO pores compared to salt, bacteria, and viruses (PureRO USA, 2019).

3.3 Summary of the benefits and drawbacks of Reverse Osmosis

In the pursuit of sustainable practices, there are always benefits and drawbacks that must be considered with old or emerging technology. As with anything, RO applications should be evaluated on a case-by-case basis for best fit and not assumed to be a best practice for any situation in need of water supplementation.

The key benefit of reverse osmosis is the low energy that it requires to desalinate sea water into fresh water. Compared to traditional methods of distilling, RO far outstrips the competition for energy used per unit of freshwater produced. Another benefit of RO is its scalability. Individual RO units can be installed in parallel or in-line with several units to rapidly increase water output. These modifications also require little change in the overall

system dynamic, other than upscaling equipment to ensure the proper pressures to overcome osmotic forces will be achieved.

One of the drawbacks to RO systems is that they require a lot of disposable products. As a membrane ages, it becomes less productive and requires more energy to produce freshwater. Each time a membrane's life is over, it must be disposed of, without any means of recycling, and a new membrane must be purchased. This life cycle of disposables leads to high recurring costs and the production of landfill waste.

Another drawback is that desalination is not yet economically competitive with fresh water harvesting. Though RO is the most energy-efficient desalination method, and thus the least expensive, it is still significantly more expensive than any sort of freshwater purification techniques (Al-Karaghoul, Kazmerski, & (NREL), 2013).

Finally, reverse osmosis is nearing its theoretical efficiency limit. Since the 1970's, seawater RO has improved from an energy consumption rate of $20 \text{ kWh} * \text{m}^{-3}$ to almost $2 \text{ kWh} * \text{m}^{-3}$ at a recovery rate of 50% today (Mazlan, Peshev, & Livingston, 2016; Elimelech & Phillip, 2011). According to Elimelech, the theoretical limit of efficiency for SWRO is $1.56 \text{ kWh} * \text{m}^{-3}$. Though there are still improvements that can be made, the technology has improved rapidly and is approaching its maximum efficiency.

3.4 Reverse Osmosis Rig at Embry-Riddle

3.4.1 *Project Goals and Requirements*

Based on typical RO setups, the following was the list of design goals made by the student team:

- | | |
|--|---|
| 1. Safety Requirements | 2. Performance Requirements |
| 1.1 Shall meet ERAU electrical standards | 2.1 Shall fit in a 5' by 2.5' cart |
| 1.2 Shall include an emergency stop button | 2.2 Shall be powered through an external power source |
| 1.3 Shall prevent over-pressurization and/or explosion | 2.3 Shall not draw more than 5kW of power |
| 1.4 Shall prevent over-amperage | 2.4 Shall produce at least 3 GPM of freshwater |
| 1.5 Shall have clearly labeled controls and meters | 2.5 Shall include filtration before RO membrane |
| 1.6 Shall have attached waterproof manual | |

3.4.2 Schematics

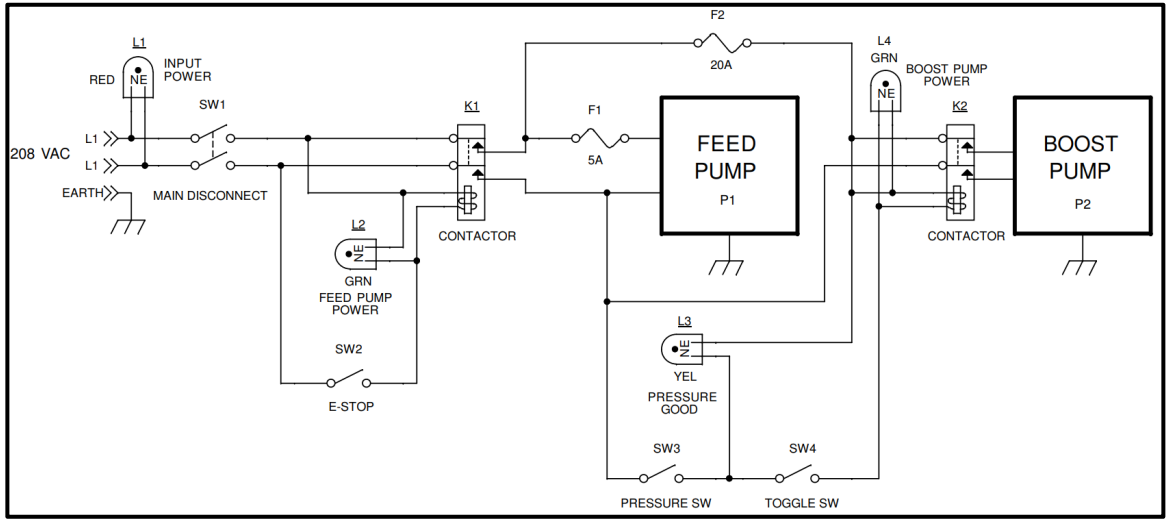


Figure 26: Electrical schematic for the ERAU test rig.

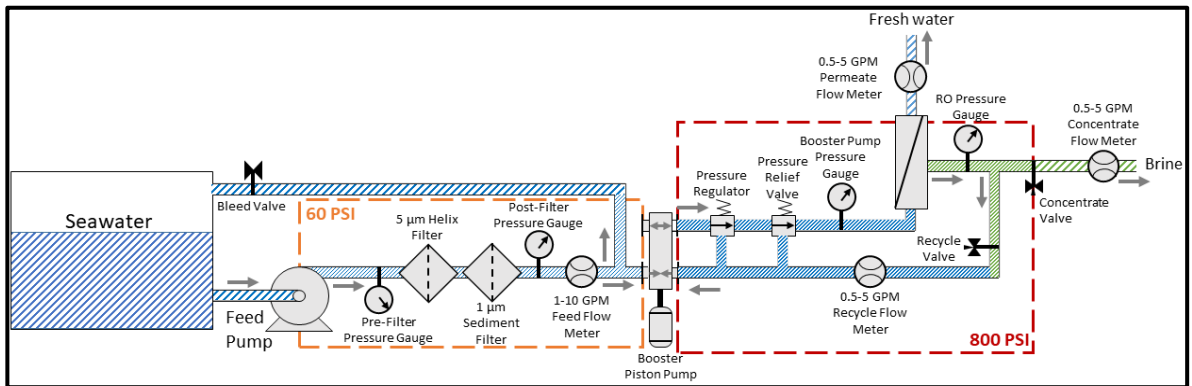


Figure 27: Schematic of the entire system.

Figure 26 and Figure 27 above illustrate the setup for a single membrane RO system. Figure 26 lays out the electrical setup, with safety precautions to prevent over-pressurization within the system and has faults in the case of water-electrical contact. Figure 27 illustrates the low pressure zone versus high pressure zone functions, in addition to flow direction and additional mechanisms needed in the system such as check valves, pressure gauges and flow meters.

3.4.3 *SolidWorks Rendition*

Figure 28 below was the final rendition of the RO Test Rig within SolidWorks. Fasteners, tubing, and parts are represented.

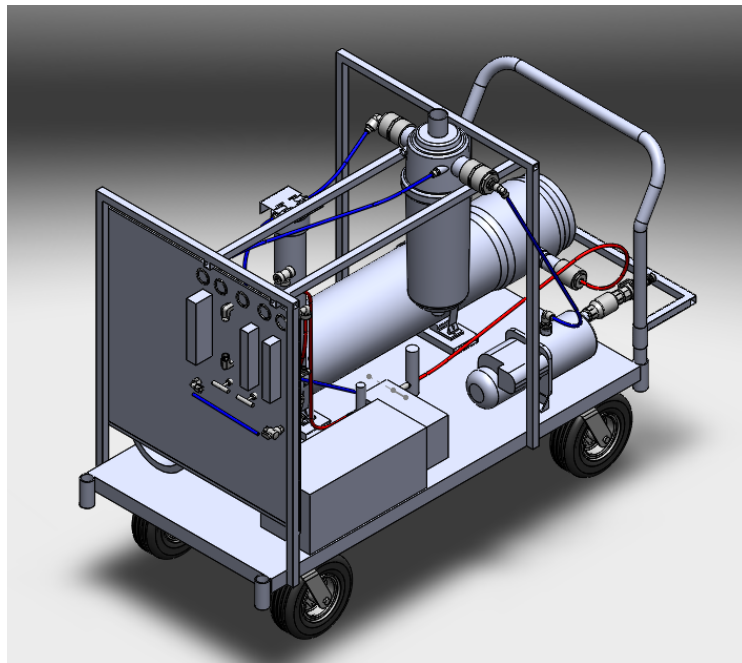


Figure 28: 3D Model of the RO Test Rig, done in SolidWorks.

3.4.4 Final Build

The final build of the RO Test Rig is seen in Figure 29. The machine is fully operational.

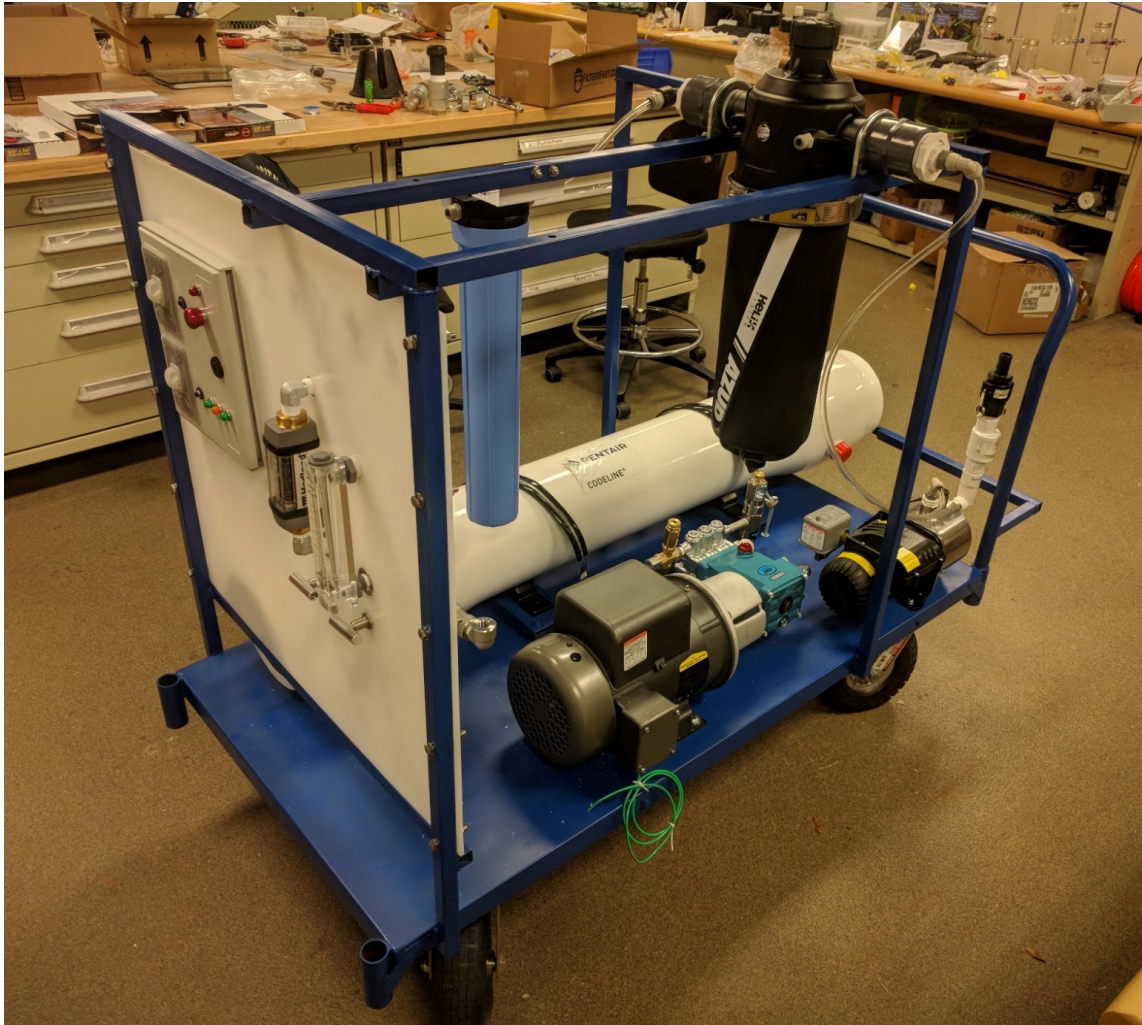


Figure 29: Physical RO Test Rig located in the Energy Systems Laboratory at ERAU.

3.5 Tampa Desalination Plant

Students from the organization Project Haiti at Embry-Riddle (Daytona Beach) have travelled to the Tampa Bay Desalination Plant to learn about desalination at the municipal scale. Because of this relationship, Tampa Bay Water was willing to share tracked data from 2016, 2017, 2018 and the early part of 2019. The 2016 and 2019 collected data are incomplete, so for completeness only 2017-2018 is included here. The photos below show a brief section of the RO unit setup at the plant.



Figure 30: Tampa Bay Desalination unit pumps, courtesy of Tampa Bay Water.



Figure 31: Tampa Bay Desalination plant reverse osmosis units.

Desalination can offer a great supplementary resource to existing freshwater resources. In Florida, there is heavy rainfall in the summer months which is why there is low or no production at the desalination plant. There is no need to desalinate during months where there is a sufficient fresh water supply. During the drier months, however, the plant has the capacity to supplement water production for the Tampa Bay area.

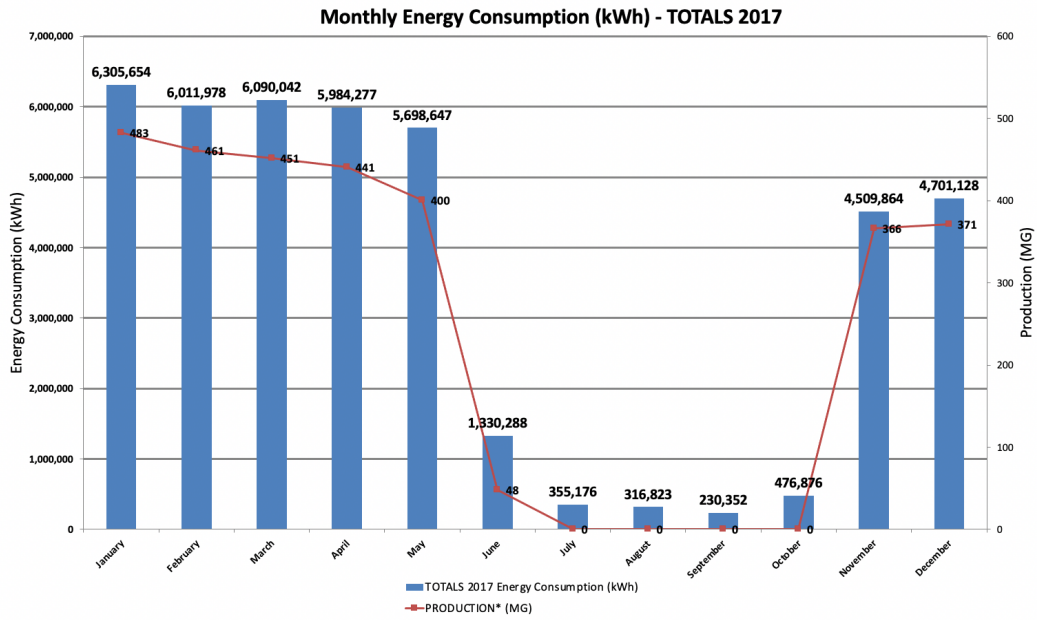


Figure 32: Water production totals in 2017. *All water sent to Tampa Bay Water.

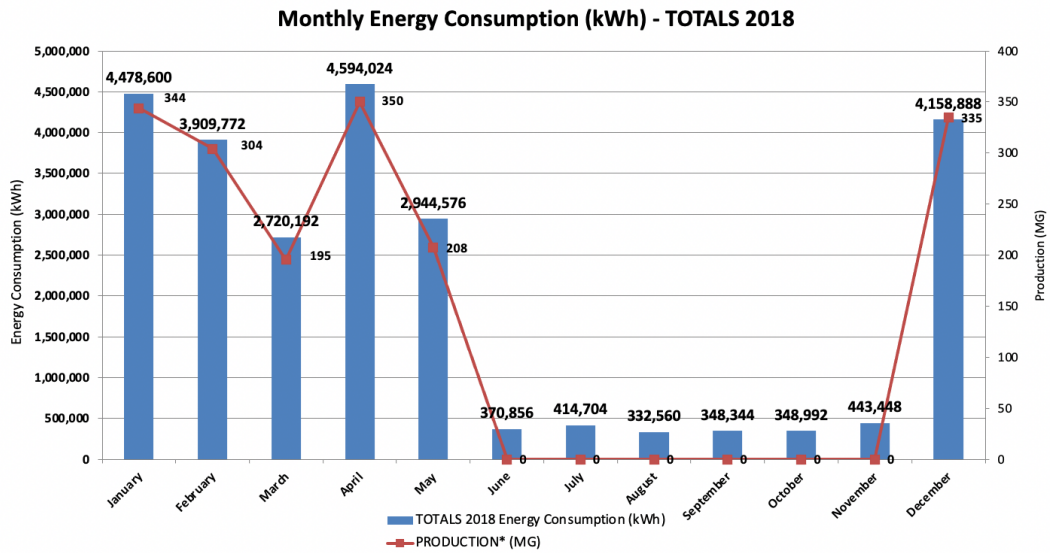


Figure 33: Water production totals in 2018. *All water sent to Tampa Bay Water.

3.6 Conclusion

In conclusion, there are many benefits to using reverse osmosis desalination as a means of producing freshwater. While there are many advances that must be made, it is a competitive model for ensuring the water security of coastal regions and other communities that may experience salt intrusion in typically freshwater aquifers. The global drive towards sustainable practices in all areas of life will push reverse osmosis towards becoming less waste-prone, but the need for freshwater for a growing global population in the midst of climate change will require growth in the use of RO.

3.7 Recommendations for Future Work in RO

Future work could include creating porous membranes that are either biodegradable or somehow able to be cleaned after use. There are some membranes that must be disposed of as toxic waste after filtering things like lead and arsenic. Even non-toxic membranes are simply disposed of as waste and sent to landfills. In an ideal sustainable solution to water scarcity, any type of permanent waste will be minimized. Finding ways to make membranes last longer and stay out of landfills will be an important step towards sustainability.

Another area of research in reverse osmosis should include powering desalination plants with renewable energy resources. The change in global climate is increasing the severity of the growing global water crisis, so creating fresh water in a way that does not

expound on this climate change is imperative. Research on energy storage or producing as much freshwater as possible during peak sunlight or wind hours as will be distributed in off-hours will help ensure that this technology does not become a detriment to the environment.

Finally, responsible management of the concentrated brine must be a priority. For now, brine is distributed back into the ocean in such ways as to not create densely salted pockets within the ocean. As desalination becomes more widely used, it will be imperative that brine distribution sites are researched and monitored to ensure that ecosystems within the ocean are not being disrupted by brine disposal.

Chapter IV

4 Vacuum Distillation

To better understand the potential energy savings of low-pressure distillation, this chapter explores the characteristics of phase-change processes, specifically the change of phase from liquid water to vapor. Due to a low number of available studies on low-pressure vaporization intended for maximizing mass transfer (which is the goal of this study), the phase-change processes of evaporation and boiling are explored in detail.

Evaporation refers to the process of liquid molecules breaking free of the surface of a liquid (Cengel & Ghajar, 2016). Boiling involves added heat that creates vapor bubbles at the surface of the heat source, which then rise to the surface of the fluid (Cengel & Ghajar, 2016). A review of the characteristics of vaporization and boiling are discussed in three categories: (1) boiling characteristics at standard pressure, (2) low-pressure boiling, and (3) mass transfer of evaporative processes at standard pressure.

4.1 Characteristics of boiling in standard pressure systems

4.1.1 *Subcooled boiling*

In an article published in 1985, Del Valle defines nine characteristics of “subcooled flow boiling.” Subcooled boiling “is characterized by the appearance of bubbles initiating from the heater surface while the bulk temperature is still below the saturation” (Yan, Bi, Lui, Zhu, & Cai, 2015). According to Yan et. Al., subcooled boiling has a higher heat

transfer efficiency and better critical heat flux performance, as confirmed by multiple experiments (Wang, 2009; Lee, 2009). The context of the study was to explore cooling nuclear reactors and is more commonly understood in applications of heat transfer applied to cooling systems such as energy-producing reactors, or heat-producing electronics. It will be important to explore how subcooling affects mass transfer, however, as this may be beneficial for high heat flux but may impact mass flux of liquid to vapor. If subcooled boiling occurs, it is likely that the vapor created at the heated surface will condense before escaping the subcooled liquid layer (Michaie, Rulliere, & Bonjour, 2019). Should this happen, it would be a waste of energy and negatively impact the energy efficiency of the system.

4.1.2 Effect of wall thickness on heat flux

At standard pressures, there are several patterns in the nucleation sites, or the areas where new bubbles will begin. The rate of nucleate boiling heat transfer at a given wall superheat increases with increasing wall thickness and increased subcooling (Del Valle M & Kenning, 1985). The patterns of nucleate boiling are important; therefore, it is important to examine whether or not increased nucleation increases mass transfer of evaporated water.

4.1.3 Activation site patterns

It was found that new activation sites are more likely near pre-existing activation sites within certain bubble radii, though new sites tend to deactivate the old sites (Del Valle M & Kenning, 1985). Bubble nucleation patterns have a large effect on the heat transfer properties and vaporization of the fluid (Michaie, Rulliere, & Bonjour, 2019).

4.1.4 Maximizing heat transfer at the heated surface

At the heated surface, “heat transfer occurs primarily by bubble-induced quenching of the wall by cold liquid” (Del Valle M & Kenning, 1985). Additionally, microlayers of evaporation have a negligible direct effect on the heat flux, but may still affect the bubble dynamics, thus having an indirect influence on the heat flux (Del Valle M & Kenning, 1985).

To maximize the mass transfer of evaporated water, while minimizing heat added to the system (or minimal heat flux from the heat source), it is important to understand the effect of nucleation and bubble formation both on the mass transfer and the heat transfer within the system.

4.2 Characteristics of boiling in low pressure systems

4.2.1 Pool boiling at low pressure

In a state-of-the-art review, authors from the University of Lyon in Villeurbanne, France performed an extensive literature review and study of pool boiling at low pressure. Pool boiling is the boiling of stationary fluids (Cengel & Ghajar, 2016). Michaie et al. point out that “despite the huge number of studies carried out on boiling, these unconventional conditions [of low pressure boiling] were rarely investigated” (Michaie, Rulliere, & Bonjour, 2019). Overall, there seem to be very few resources available that analyze low pressure boiling and its effect on the mass transfer of evaporated water.

To better understand the heat transfer properties of low-pressure pool boiling for applications such as electronics cooling, a study was conducted at the University of California, Berkeley. It was discovered that “the characteristics of pool boiling of water at low pressure are much different from pool boiling at atmospheric pressure” (McGillis & Carey, 1991). To further understand the behavior of water at lower pressures, several experiments were conducted to see how the heat transfer efficiency could be improved. This included altering the surface texture and surface material properties.

4.2.2 Heat transfer characteristics

Michaie et al. (2019) describe the heat transfer characteristics of low-pressure boiling. They studied the conditions of *boiling*, which requires a heat source, and it is at

this heat source that all the nucleation sites occur. As a bubble grows at the heat source wall there is a sudden drop in temperature. Likewise, the gradual reheating of the wall occurs simultaneously with the wait period between bubble growths. Compared to typical boiling conditions, low pressure boiling is “characterized by a higher minimum superheat to initiate a bubble nucleation from a given cavity, the presence of large wall temperature fluctuations with time in intermittent boiling, as well as lower heat transfer coefficient and critical heat flux” (Michaie, Rulliere, & Bonjour, 2019). This “degraded heat transfer” is, by most authors, claimed to be due to the low density of active nucleation sites. It is not how many bubbles are growing per site, instead the important degrading factor is that there are fewer sites of nucleation at all (Michaie, Rulliere, & Bonjour, 2019). One way that improves the heat transfer in low pressure pool boiling is to activate a greater number of cavities where the bubbles can nucleate (Michaie, Rulliere, & Bonjour, 2019). This indicates that the material properties of the boiling surface are quite important and should not be neglected in the design of a boiling apparatus.

4.2.3 Bubble dynamics

Bubble dynamics at low pressure differ from standard pressure boiling. Depending on the subcooling degree, it is typical to see “mushroom” shaped bubbles that result from the unique dynamics of the low-pressure system. As an initial bubble departs from the heat source, a vapor mass may grow without the nucleation of an entirely new bubble. This creates a “mushroom-like” shape of vapor. If the liquid beyond the heat source is too cool,

it is also likely for the bubble to collapse within the cooler liquid before escaping as vapor beyond the fluid surface. As these effects are often studied with heat transfer optimization in mind, this behavior may not generally be detrimental. However, as the goal here is water purification through distillation, having energy lost on vapor that condenses before escaping will certainly have negative effects on the efficiency of the distillation process.

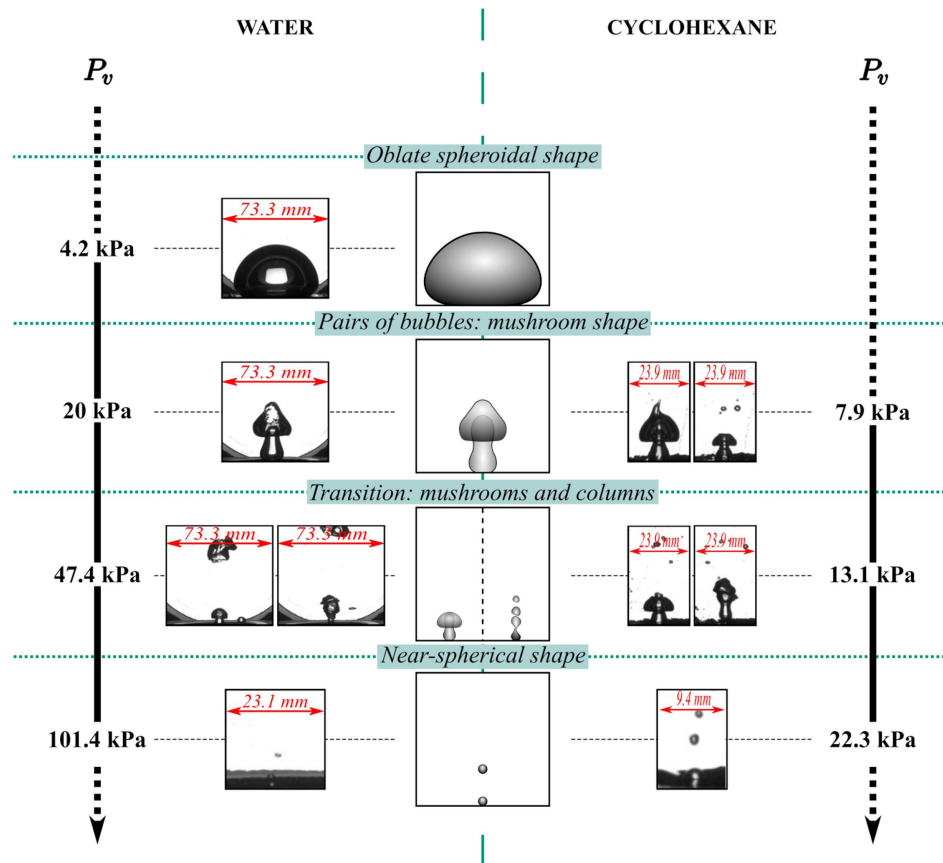


Figure 34: Illustrates the progression of bubble dynamics of water and cyclohexane at various pressures (Michaie, Rulliere, & Bonjour, 2019).

The size of vapor bubbles also changes under lower pressure conditions. As a result of the low pressure, “the bubbles that form on a surface and their departure diameters are large” with respect to the “container, heated surface, and bubble diameter at higher pressures” (McGillis & Carey, 1991). The large bubble diameters present some issues to the heat transfer efficiency from a heated surface. As the bubbles depart, they disturb the water, mixing it, consequently removing some of the already-heated water from the surface of the heating element. This creates a longer waiting period for the next bubble formation as the water at the heating element must be reheated. Additionally, a large vapor bubble, in smaller containers, is actually enough to change the vaporization pressure of the entire system. This means that the vapor pressure increases, which can cause other already-formed bubbles to collapse within the fluid or create a longer heating time for the water to overcome the vaporization pressure. Finally, because of the large-diameter bubbles created at lower pressures, much larger superheats are generally needed, there are fewer bubble activation sites, and these factors contribute to the longer waiting time (McGillis & Carey, 1991).

In summary, Michaie et al. (2019) break down the bubble dynamics of a low-pressure system into three steps:

1. Natural convection takes place, creating a thermal boundary layer by conduction close to the heated surface, then by natural convection. This leads to a long waiting time without any bubble nucleation.

2. This is followed by “rapid growth and departure of a large bubble from an activated nucleation site.”
3. Finally, several bubbles of variable sizes and frequencies nucleate everywhere on the heated wall. (Michaie, Rulliere, & Bonjour, 2019)

4.2.4 *Surface finish and activation sites*

Surface finish makes a substantial impact on the efficiency of low-pressure boiling. A key to increasing the heat transfer efficiency is increasing the number of activation sites, or places where new bubbles will nucleate. It was found that at “a wall superheat of 25 degrees C, an increase in surface roughness from 0.16 to 5.72 μm rms provides about a 100% increase in heat flux” (McGillis & Carey, 1991). This shows how drastic the effect of surface roughness can be. However, activation sites are not solely based on the surface texture. According to McGillis, “bubble nucleation also depends on nucleate embryos (absorbed gases and vapors), vapor density, heat of vaporization, and surface tension.” To optimize heat transfer, it is important to consider all of these factors.

Fins in addition to the heat plate

Adding fins to the heated surface significantly extends the nucleate boiling range beyond that of a flat plate (McGillis & Carey, 1991). This benefit is not indefinite, however. The research found that beyond a certain fin length, per the fin length-to-width ratio, the performance did not continue to improve. Part of the improvement of the boiling

performance with fins is due to the added cavity sites at the base of the fins. Long intermittent waiting time is part of the low efficiency of low-pressure boiling. The added cavity sites at the base of the fins make a significant difference, in addition to the added heat transfer qualities of the fins.

The space between added fins, referred to as a “fin gap,” also impacts the heat transfer performance. Fins with identical heating areas that were placed closer together had better heat transfer efficiencies. With a flat plate, the bubbles escaping the water surface mix the water, decreasing the temperature of the water at the heated surface. It seems that the closer the fins are placed, the less the water mixes near the base of the fins and at the heated surface, resulting in less waiting time between bubble departures (McGillis, 1991; Niro, 1990).

4.2.5 Non-homogeneity

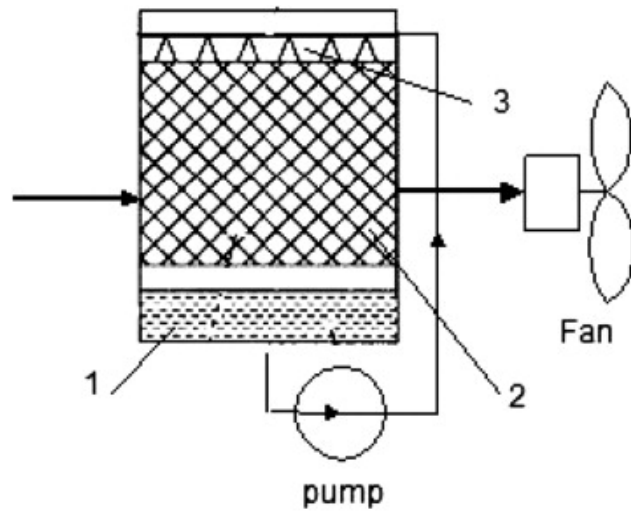
First found by Ponter and Haigh in 1969, and confirmed again by Schnabel et al. in 2008, the “influence of the liquid height over the heated surface on the low pressure boiling heat transfer” is non negligible and must be factored into calculations (Michaie, Rulliere, & Bonjour, 2019). Additionally, the pressure and subcooling degree cannot be considered homogeneous around low-pressure bubble formations. First, the vapor created by the bubble has large enough impacts on the system pressure that as the bubble is forming, the pressure in the system is actively changing, simultaneously changing the vapor pressure of the liquid as well. The subcooling degree cannot be considered homogenous, because as

the bubbles form, the temperature at the wall drops drastically, and the cooler water fills in behind the bubble, often causing the vapor to condense before it ever escaped the liquid. This combination of circumstances leads to nonhomogeneous behaviors within the fluid.

4.3 Mass transfer at standard pressure

4.3.1 HVAC Applications

Mass transfer is not as heavily studied under boiling conditions because many of the studies on boiling are interested in the heat transfer characteristics. Studies focused on cooling properties of air conditioning or other cooling systems do look into mass transfer, however. Since the latent heat of water is so high, it is common to use water as a coolant in air-conditioning. The phase-change process of water changing from liquid to vapor pulls heat away from the system (Fouda & Melikyan, 2010). A direct evaporative cooler humidifies air with cool water, which absorbs heat from the air (Fouda & Melikyan, 2010). The humidified and cooled air is pumped into the space, as shown in Figure 35.



(1) water basin (2) pad material (3) water distribution system

Figure 35: Schematic of a direct evaporative cooler (Fouda & Melikyan, 2010).

Though the goal of the research here is not in heating and cooling large spaces, the research done by engineers in the HVAC community is beneficial as it relates mass transfer and heat transfer within a system.

4.4 A Laboratory Example Illustrating the Complexity of Low Pressure Phase Change

An interesting experiment involving phase change, low pressure, and heating water to an elevated temperature is used to clearly describe physics of vacuum phase change. The experimental setup includes a small cup of water heated to approximately 70C. The cup of water was placed in an aluminum vacuum chamber and a vacuum pump was used to reduce pressure from atmospheric to -14.0 psi in approximately 20 seconds. Photos at STP and after, or during vacuum draw is shown below.



Figure 36: Shown above is a laboratory experiment of low-pressure vaporization.

Inside the sealed vacuum chamber is a glass jar with warmed water inside of it.

What occurred was water bubbling up and overflowing the container inside the vacuum chamber as pressure dropped. Some conclusions can be drawn to delineate between three common forms of phase change: boiling, evaporation, and cavitation.

1. This was *not* boiling because there is no heating surface.
2. This was *not* evaporation because nucleation sites were clearly visible from within the liquid container. The mass transfer was not only at the surface.
3. This *was* cavitation because the water experienced a rapid pressure drop at sufficient temperature to change phase.

This example illustrates the complexity of fresh water phase change phenomenon for different boiling chamber designs.

4.5 Summary

The behavior of vaporizing water below atmospheric pressure is not completely understood by researchers. Because of this, it is helpful to have a well-rounded understanding of boiling and evaporative mass transfer characteristics under the conditions in which they have been studied. With the knowledge acquired through other researchers, the patterns between standard-pressure mass transfer and boiling characteristics, and low-pressure vaporization can be compared and analyzed to draw conclusions about the patterns of mass transfer at low pressures.

4.6 Thesis statement

Low pressure distillation has potential to generate a greater fresh water mass, for the same input energy, compared to distillation at STP. A model is developed that relates temperature, pressure, and input heat transfer to the freshwater mass output. The primary result is the ability to predict freshwater production from low-pressure vaporization.

Chapter V

5 Boiling Models and Predictions

The goal of this chapter is to present models of low-pressure boiling from these conventional categories:

1. Rohsenow's boiling framework at standard pressure,
2. Michalek's low pressure boiling considerations with pool boiling, bubble dynamics, and head height
3. Evaporative mass transfer in an HVAC context
4. Evaporative mass transfer in a solar basin

By analyzing the models developed by these researchers, it is possible to, with certain assumptions, create a predictive model for systems operating under low pressure. Proposed experimental setups to verify the model are included in chapter 6.

5.1 Conventional Mass Transfer Models

5.1.1 Pool Boiling at Standard Pressure

Calculations on boiling phenomenon require knowledge of many of the experimental parameters. Based on the range of circumstances, different constants and equations will be used (Cengel & Ghajar, 2016). The most widely used correlation for

nucleate boiling heat transfer is known as the Rohsenow equation (Cengel, 2016; Rohsenow, 1952):

$$\dot{q} = \mu_l h_{fg} \left[\frac{g(\rho_l - \rho_v)}{\sigma} \right]^{1/2} * \left[\frac{c_{pl}(T_s - T_{sat})}{C_{sf} h_{fg} Pr_l^n} \right]^3 \quad (1)$$

where:

\dot{q} = nucleate boiling heat flux, W/m²

μ_l = viscosity of the liquid, kg/m·s

h_{fg} = enthalpy of vaporization, J/kg

g = gravitational acceleration, m/s²

ρ_l = density of the liquid, kg/m³

ρ_v = density of the vapor, kg/m³

σ = surface tension at the liquid-vapor interface, N/m

c_{pl} = specific heat of the liquid, J/kg·°C

T_s = surface temperature of the heater, °C

T_{sat} = saturation temperature of the fluid, °C

C_{sf} = experimental constant, dependent on surface-fluid combination

Pr_l = Prandtl number of the liquid

n = experimental constant, dependent on the fluid

As seen in Figure 37, at standard pressure, the nucleate boiling regime is considered to be between 5 degrees Celsius and 30 degrees Celsius excess temperature. Nucleate

boiling refers to the phase of the boiling regime where bubbles form at an increasing rate. The nucleate boiling range can also be split into two categories: first, from 0 to 10 degrees Celsius, isolated bubbles are formed but typically dissipate quickly in the liquid. From 10 to 30 degrees, the bubbles form steady vapor columns and reach the surface of the fluid. Within the nucleate boiling range (0 to 30C), the rate of heat transfer (similar to low pressure boiling) depends strongly on the number of active nucleation sites, and the rate of bubble formation at each site (Cengel & Ghajar, 2016). The Rohsenow equation was developed on extensive experimental data, and accounts for as many of these variables as possible to predict the rate of heat transfer.

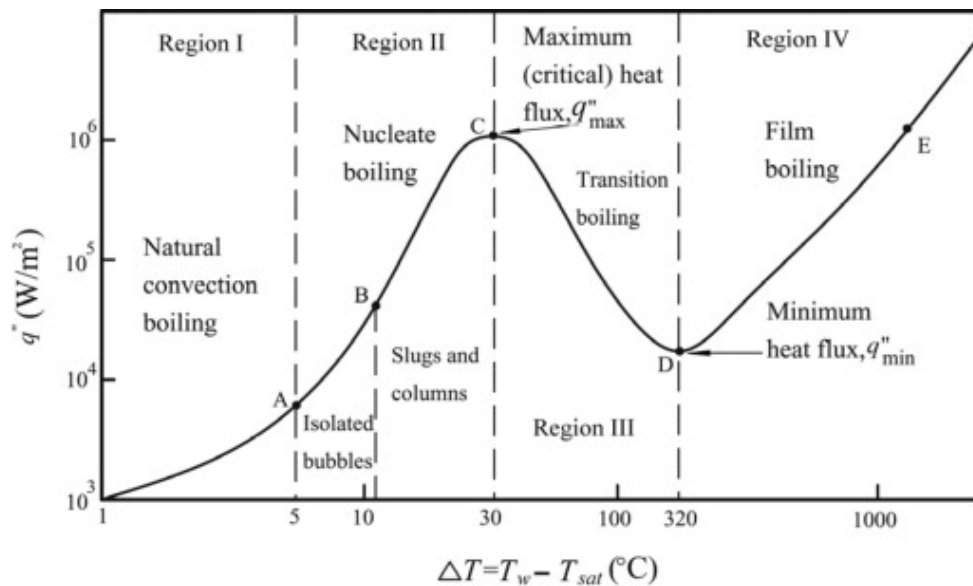


Figure 37: Typical boiling curve for water at 1atm (Faghri & Zhang, 2006).

For water, the surface tension, σ , depends on the temperature of the water. Table gives a range of the values for surface at different temperatures.

**Table 5.1: Surface tension at the liquid-vapor interface
of water (Cengel & Ghajar, 2016).**

TEMPERATURE, CELSIUS	σ, N/M
0	0.0757
20	0.0727
40	0.0696
60	0.0662
80	0.0627
100	0.0589
120	0.0550
140	0.0509
160	0.0466
180	0.0422
200	0.0377
220	0.0331
240	0.0284
260	0.0237
280	0.0190
300	0.0144
320	0.0099
340	0.0056
360	0.0019
374	0.0

Values for C_{sf} and n vary based on the fluid and the material of the surface. Table shows a sample of values of each based on the type of surface paired with water.

Table 5.2: Values of C and n for various surface-fluid combinations (Bergman, Incropera, DeWitt, & Lavine, 2011).

FLUID-SURFACE COMBINATION	C_{sf}	N
WATER-COPPER		
· SCORED	0.0068	1.0
· POLISHED	0.0128	1.0
WATER-STAINLESS STEEL		
· CHEMICALLY ETCHED	0.0133	1.0
· MECHANICALLY POLISHED	0.0132	1.0
· GROUND AND POLISHED	0.0080	1.0
WATER-BRASS	0.0060	1.0
WATER-NICKEL	0.006	1.0
WATER-PLATINUM	0.0130	1.0

The Rohsenow equation is not typically applied directly in low-pressure applications because pressure is not accounted for. It is, however, fundamental to the

understanding of pool boiling heat transfer correlations at standard pressure. With manipulations made in the final chapter, it can be seen how this relates to low-pressure behaviors.

At standard pressure, the following equation relates the heat flux calculated through Rohsenow's equation to mass transfer of evaporated water.

$$\dot{Q} = A * \dot{q} \quad (2)$$

Equation 2 relates heat flux to heat transfer, \dot{Q} , by incorporating the surface area of the heating element, A (Cengel & Ghajar, 2016; Bergman, Incropera, DeWitt, & Lavine, 2011).

$$\dot{m} = \frac{\dot{Q}}{h_{fg}} \quad (3)$$

Finally, the mass transfer, \dot{m} , is calculated in Equation 3 by dividing heat transfer by the enthalpy of vaporization (Cengel & Ghajar, 2016; Bergman, Incropera, DeWitt, & Lavine, 2011).

5.1.2 Low-Pressure Pool Boiling Model

“Low pressure” boiling is defined as “boiling at pressures below the atmospheric pressure ($P_v = 101.4$ kPa, $T_v = 100$ degrees C)” (Michaie, Rulliere, & Bonjour, 2019; McGillis & Carey, 1991; Van Stralen, Cole, Sluyter, & Sohal, 1975; Giraud, Rulliere, Toubanc, Clause, & Bonjour, 2015; Zajaczkowski, Halon, & Krolicki, 2016). There are many models for simulating heat transfer of boiling at standard temperatures and pressures,

but models of low-pressure systems are much less researched (Michaie, Rulliere, & Bonjour, 2019).

For a low-pressure system, the pressure at the level of the heated surface, P_{wall} , should be taken into account. At standard pressure, and even in many studies at sub atmospheric pressures, the head height of the water is not considered. However, the pressure created by the head height, H_l , affects the pressure at the heated wall, in turn affecting the bubble nucleation at the heated surface (Michaie, Rulliere, & Bonjour, 2019). Equation (2) describes the pressure at the heated surface.

$$P_{wall} = P_v + \rho_l(t_{l,bulk})gH_l \quad (4)$$

where P_v is the vapor pressure at the free surface, ρ_l is the density of the liquid, $t_{l,bulk}$ is the temperature of the liquid within the static column of water above the examined heated surface, g is the gravitational constant, and H_l is the height of the liquid column.

In low-pressure conditions, it is possible for the wall pressure to approach the triple point pressure, P_t . This leads to, at low liquid heights, a case where the bubble diameter can grow so large that it actually exceeds the height of the fluid. This is no longer considered pool boiling, so all the following equations assume that the height of the liquid column is relatively high (Michaie, Rulliere, & Bonjour, 2019). The following equations illustrate this phenomenon.

If the pressure at the heated surface is close to the triple point, P_t ;

$$P_{wall} \approx P_t \quad (5)$$

However, it is true that

$$P_v \geq P_t \quad (6)$$

so, to satisfy equation (3), it must also be true that

$$P_v \approx P_t \quad (7)$$

and

$$P^{static} = \rho_l(T_{l,bulk})gH_l \ll P_t \quad (8)$$

where P^{static} is the static head induced by the liquid column over the heated surface.

Another parameter examined in boiling phenomena is the capillary length, L_c . The capillary length is used to approximate the diameter of a bubble upon its departure from a fluid. It is calculated based on the resultants of buoyancy and surface tension (σ) forces, and the equation is shown below:

$$L_c = \sqrt{\frac{\sigma}{g(\rho_l - \rho_v)}} \quad (9)$$

This equation does not necessarily work in low-pressure applications, however. Inertia and the Marangoni force should be considered, as well as the buoyancy and surface tension. Because the bubble diameter is so large, it affects the vapor density, ρ_v (Michaie, Rulliere, & Bonjour, 2019). The density ratio, shown below, helps to illustrate that for the same volume of liquid vaporized, a higher value density ratio produces a larger volume of

vapor, and the density ratio can be used as an estimate to indicate the relative size of bubbles (Michaie, Rulliere, & Bonjour, 2019).

$$\text{Density Ratio: } \frac{\rho_l}{\rho_v} \quad (10)$$

Again, models exist for simulating heat transfer of boiling at standard temperatures and pressures, but models of low-pressure systems are hard to find (Michaie, Rulliere, & Bonjour, 2019). The final chapter of this paper estimates the energy savings of a low-pressure system based on these known standard-pressure calculations.

5.1.3 Evaporative Cooling; Heat and Mass Transfer Model in HVAC

Many cooling systems use water as the working fluid for heat transfer due to its accessibility, low cost, and lack of harmful chemicals that are found in many other coolants. A simple analysis of an evaporative cooler was conducted with the following assumptions:

1. The heat and mass transfer process are unsteady and performed in one dimension.
2. The pad material is easily and uniformly wetted, where the pad material is the surface area under examination. Air is passed through the pad material, thus humidifying and cooling the air.
3. Any water film on the pad surface is very thin.
4. The thermal properties, density, and specific heat of the air are constant (Fouda & Melikyan, 2010).

The coordinate system and schematic of the problem are shown below in Figure 38.

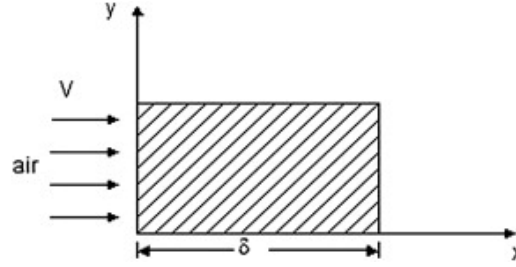


Figure 38: Schematic of evaporative cooler analysis (Fouda & Melikyan, 2010).

The analysis is set up with four governing equations and a set of boundary conditions. The governing equations for moist air are:

Mass continuity equation

$$\rho \frac{\partial u}{\partial x} = m_v \quad (11)$$

Momentum equation in the x direction

$$\rho \frac{\partial u}{\partial t} + \rho u \frac{\partial u}{\partial x} = \rho \frac{\partial^2 u}{\partial x^2} + m_v u \quad (12)$$

Energy conversion equation

$$\rho c_p \frac{\partial T}{\partial t} + \rho u c_p \frac{\partial T}{\partial x} = k \frac{\partial^2 T}{\partial x^2} - q_v \quad (13)$$

Mass conservation equation of the moisture in the air

$$\rho \frac{\partial d}{\partial t} + u \frac{\partial d}{\partial x} = D \frac{\partial^2 d}{\partial x^2} - \frac{m_v}{\rho} \quad (14)$$

where d is the air humidity ratio kg_w/kg_a , T is air temperature in Kelvin, D is the effective thermal diffusion coefficient of air in m^2/s , m_v is the mass source term in $\text{kg}/\text{m}^3\text{s}$, and q_v is

the heat source term (Fouda & Melikyan, 2010). These equations are then subject to the boundary conditions listed below:

Initial conditions:

$$\begin{cases} T(x, 0) = T_1 \\ d(x, 0) = d_1 \end{cases} \quad (15)$$

Boundary conditions:

$$T(0, t) = T_1 \quad (16)$$

$$d(0, t) = d_1 \quad (17)$$

$$\left. \frac{\partial T}{\partial x} \right|_{x=\delta} = 0 \quad (18)$$

$$\left. \frac{\partial d}{\partial x} \right|_{x=\delta} = 0 \quad (19)$$

Then, the mass source, m_v , and heat source, q_v , can be found using the following (Hawladar & Liu, 2002):

$$m_v = k_a(d_s - d) \quad (20)$$

$$q_v = k_a(h_s - h) \quad (21)$$

where k_a is the volumetric mass transfer coefficient for the padding of the material, in $\text{kg/m}^3\text{s}$. It is possible that for an analysis without padding material, these terms will drop out entirely. However, the full analysis is included so that faulty assumptions can be avoided.

Next, “the enthalpy, wet-bulb temperature, and humidity ratio of moist air can be determined from the following formulas” (Fouda & Melikyan, 2010):

$$h = c_p t + d(2500 + 1.84t) \quad (22)$$

$$t_{wb} = 2.265(1.97 + 4.3t_{db} + 10000d)^{0.5} - 14.85 \quad (23)$$

where:

$$d = \frac{0.622p_v}{p_{atm} - p_v} \quad (24)$$

Saturated water vapor creates an additional pressure on the evaporative surface. In this application, the surface is assumed to be a honeycomb humidifier (Fouda & Melikyan, 2010). The pressure added by the saturated water vapor is calculated with this formula:

$$p_{st} = e^{\left(23.196 - \frac{3816.44}{T - 46.13}\right)} \quad (25)$$

The “mass diffusion coefficient of vapor in the air” is found using the following equation (Fouda, 2010; Zhang, 2003):

$$D = 2.256 \left(\frac{T_a}{256}\right)^{1.81} \times 10^{-5} \quad (26)$$

Finally, the cooling efficiency, also known as the saturating efficiency, can be found with formula 25:

$$\eta = \frac{t_1 - t_2}{t_1 - t_{wb}} \quad (27)$$

Because these formulas were designed for standard pressure and temperature situations, they cannot be directly used in low-pressure applications.

5.1.4 *Evaporative Mass Transfer Model at Standard Pressure*

In multiple applications globally, researchers have investigated the low-energy consumptive process of desalination through evaporative stills. In these systems, saline water is placed into enclosed basins that heat the water through solar radiation. Freshwater evaporates and condenses on the lid of the basin. In some cases, they are multiple stages, so that each stage of evaporation gets the water progressively purer (Patel, Markam, & Maiti, 2019).

By assuming that the solar still is horizontal (though the top of the basin is typically angled so that the condensed water flows downward), the calculations for the rate of heat transfer from the water surface to the top of the glass cover can be assumed as follows:

$$\dot{q}_{cw} = h_{cw}(T_{water} - T_g) \quad (28)$$

where h_{cw} can be determined from the following relations;

$$h_{cw} = C(G_r P_r)^n \frac{K_v}{d_f} \quad (29)$$

where d_f is the spacing between the surface of the water and the top glass cover (meters), K_v is the thermal conductivity of the water in the vapor phase, C and n are constant coefficients, and G_r and P_r are the Grashof and Prandtl numbers, respectively (Patel, Markam, & Maiti, 2019).

The partial saturated vapor pressure at water temperature can be given as (Patel, Markam, & Maiti, 2019);

$$P_{water} = \exp \left(25.317 - \frac{5144}{T_{water} + 273.15} \right) \quad (30)$$

and the partial saturated vapor pressure at the temperature on the bottom of the top glass cover is calculated with the following:

$$P_g = \exp \left(25.317 - \frac{5144}{T_g + 273.15} \right) \quad (31)$$

h_{ew} can be found with the following (Cooper, 1973):

$$h_{ew} = 16.273 * 10^{-3} h_{cw} * \frac{P_{water} - P_g}{T_{water} - T_g} \quad (32)$$

Finally, with the know values of T_{water} and T_g , the hourly distillate produced, \dot{m}_{ew} can be calculated as (Patel, Markam, & Maiti, 2019):

$$\dot{m}_{ew} = \frac{\dot{Q}_{ew}}{h_{fg}} * 3600 = \frac{h_{ew}(T_{water} - T_g)}{h_{fg}} * 3600 \quad (33)$$

5.2 Creating a Comprehensive Model for Low Pressure

The created model incorporates the wider knowledge base of boiling at standard temperature and pressure. In the conclusion additional information about mass transfer knowledge of evaporative processes at standard pressure and the current knowledge on the effects low-pressure boiling are incorporated.

The modeling has been done within MATLAB. The conditions are set so that the models are running in nucleate boiling conditions. This means the temperature is low enough that critical heat flux is not achieved, but high enough that there would be nucleate boiling in “real” conditions (excess heat up to ten degrees above the vaporization temperature at the indicated pressure).

The settings of all variables within the simulations are included here in graphical form. System pressure, fluid properties such as surface tension behavior, density, specific heat, viscosity, and temperature are all be accounted for.

Current, widely used boiling models still have errors of up to 50% under variable conditions (Cengel & Ghajar, 2016). To minimize the errors of the developed model, defining the limitations and assumptions is critically important.

5.3 Theoretical Model Implementation Numerically

Even the most used boiling models can have errors of up to 50%, so assumptions and limitations are listed below to limit error (Cengel & Ghajar, 2016).

5.3.1 Assumptions

The numerical modeling assumptions are listed below:

- Assume that the binary diffusion coefficient for fresh water is the same as saltwater, since the water no longer has salt content once it diffuses.
- Assume that if there is salt content in the water vapor that it is negligible.
- Assume that the Rohsenow equation predicts heat transfer and mass transfer accurately in low pressure conditions. These models were developed under the restriction that there was excess heat in the system, meaning that as long as the temperature was above the vaporization temperature at a given pressure, the heat transfer and mass transfer is recorded.

5.3.2 Limitations of the Model

The following are limitations of the numerical model:

- The values used are all from fresh water tables.
- Some of the variables within the Rohsenow equation approach zero above 370 degrees Fahrenheit. For this reason, the model will not exceed excess temperatures of 10 degrees Celsius to avoid inaccuracy.
- The model does not account for any losses in the heat transfer or mass transfer process.

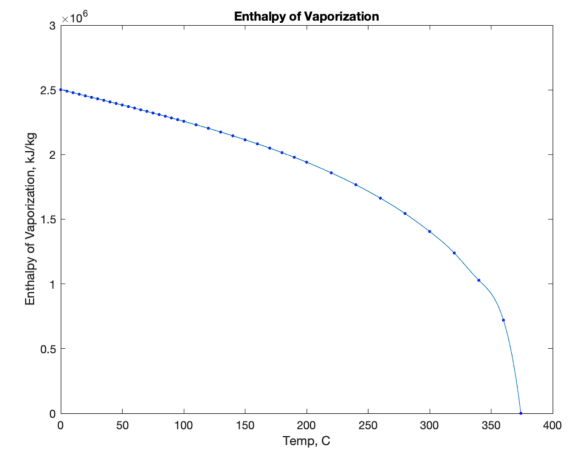
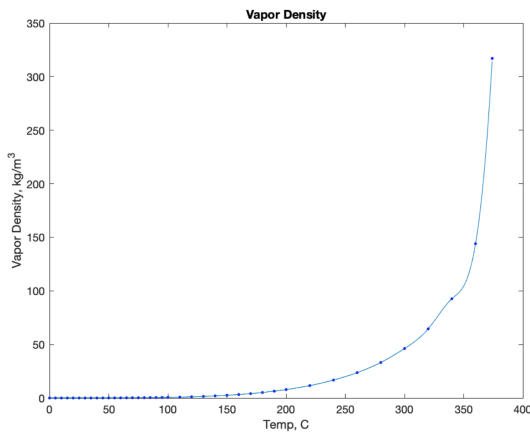
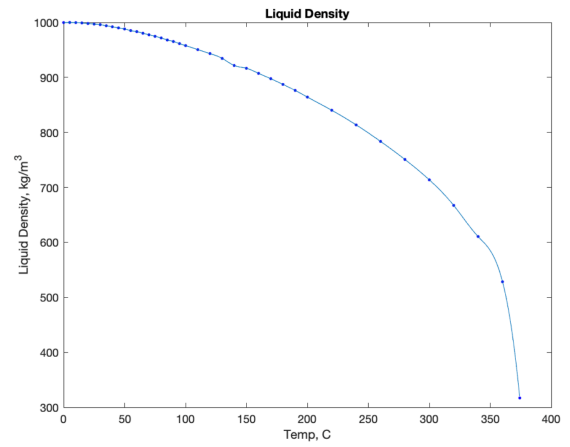
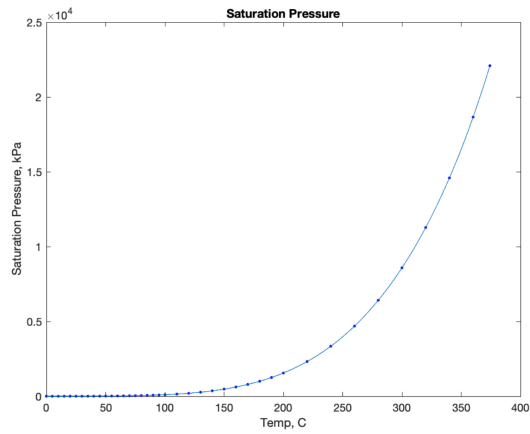
5.3.3 Mathematical Model Parameters

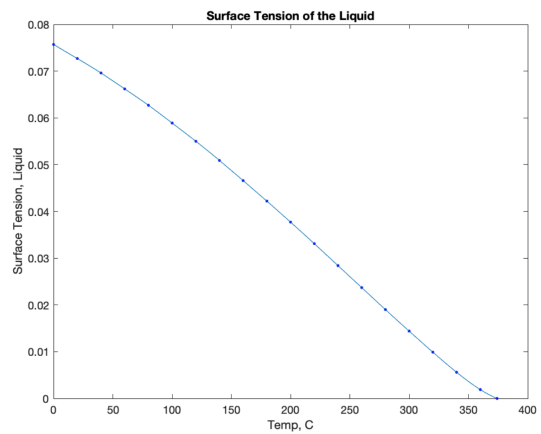
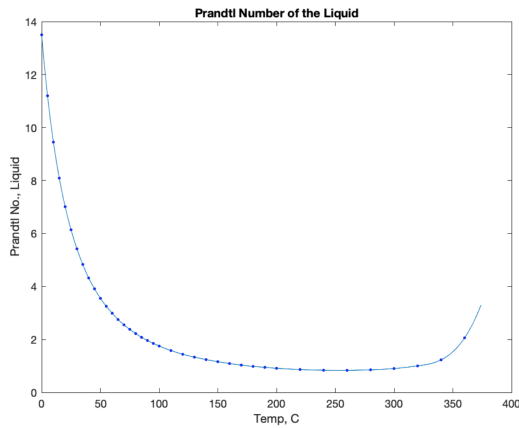
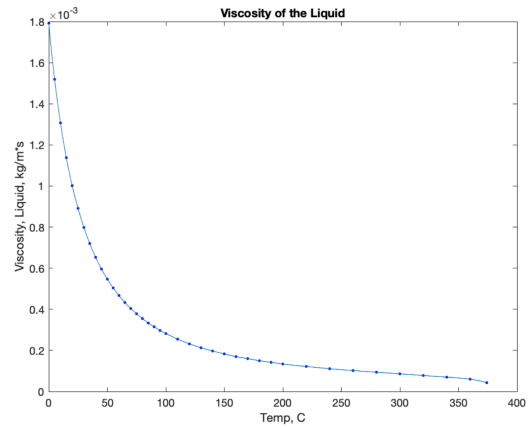
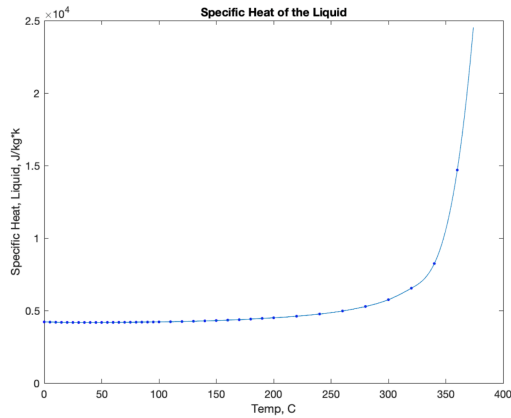
The parameters of the numerical model are included in Table below. Variables listed as “temperature dependent” are shown in section 5.3.4 in graphical form.

Table 5.3: Values of Fresh Water.

Variable	Description	Value
\dot{q}	nucleate boiling heat flux, W/m^2	Determined with the Rohsenow equation
μ_l	viscosity of the liquid, $\text{kg}/\text{m}\cdot\text{s}$	Temperature dependent
h_{fg}	enthalpy of vaporization, J/kg	Temperature dependent
g	gravitational acceleration, m/s^2	$9.81 \text{ m}/\text{s}^2$
ρ_l	density of the liquid, kg/m^3	Temperature dependent
ρ_v	density of the vapor, kg/m^3	Temperature dependent
σ	surface tension at the liquid-vapor interface, N/m	Temperature dependent
c_{pl}	specific heat of the liquid, $\text{J}/\text{kg}\cdot^\circ\text{C}$	Temperature dependent
T_s	surface temperature of the heater, $^\circ\text{C}$	Independent Variable
T_{sat}	saturation temperature of the fluid, $^\circ\text{C}$	Pressure dependent
C_{sf}	experimental constant, dependent on surface-fluid combination	Water-Mechanically Polished stainless steel: 0.0130 (Bergman, Incropera, DeWitt, & Lavine)
Pr_l	Prandtl number of the liquid	Temperature dependent
n	experimental constant, dependent on the fluid	1 (Bergman, Incropera, DeWitt, & Lavine, 2011)

5.3.4 Model Prediction Results for Properties of water from 0 to 374 degrees





5.4 Numerical Model Results

The model shown below in Figure 40 assumes that the Rohsenow equation can be applied to low-pressure analysis so long as only the nucleate phase is analyzed. Though the nucleate boiling regime spans up to 30 degrees excess temperature as seen in Figure 39, the models only go up to 10 degrees Celsius of excess temperature because the results up to 30 degrees did not appear to be physically realistic. Figure 40 shows the estimated

heat and mass transfer characteristics of water at a range of temperatures from 0 to 10(C) of excess temperature, T_{excess} .

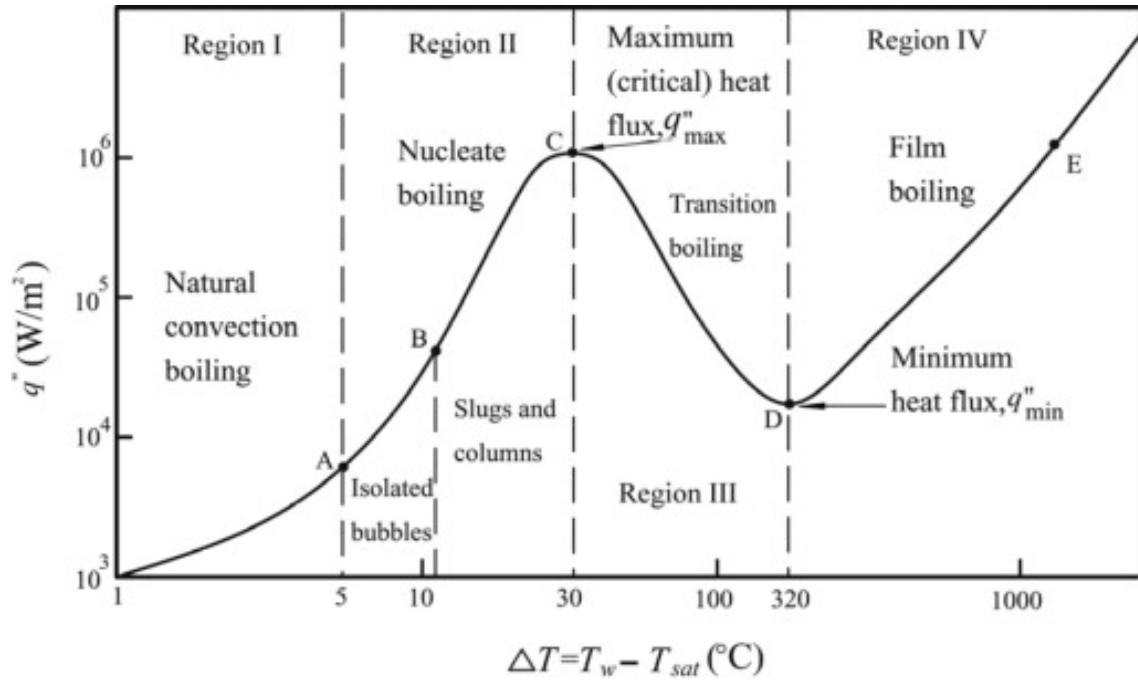


Figure 39: Boiling curve for water at 1atm (Faghri & Zhang, 2006).

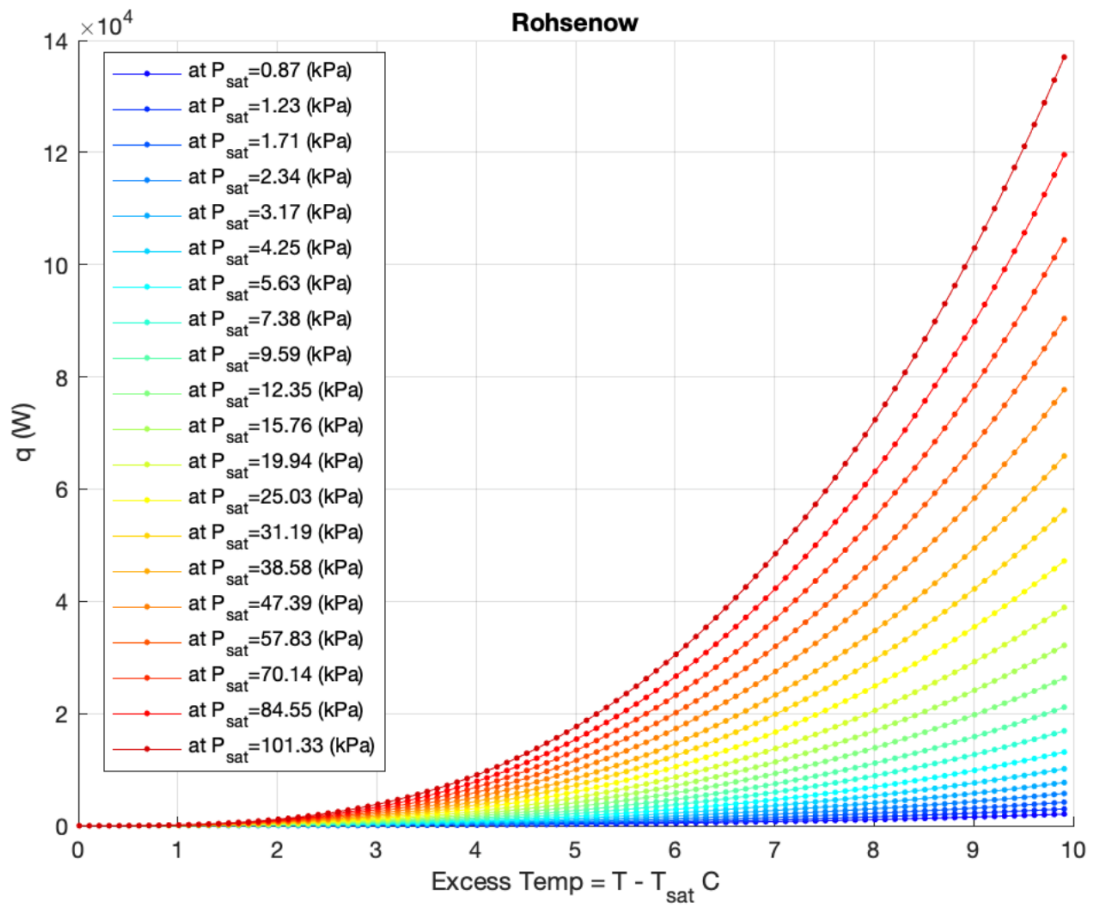


Figure 40: Heat transfer as a function of excess temperature.

Figure 40 shows heat transfer as a function of excess temperature at a range of sub atmospheric pressures down to 0.87kPa, all the way up to atmospheric pressure at 101.33kPa. For reference, 0.87kPa is designated a medium vacuum (Fradette & Jones, 2016). This figure shows that increasing the temperature of the water requires less energy at lower temperatures.

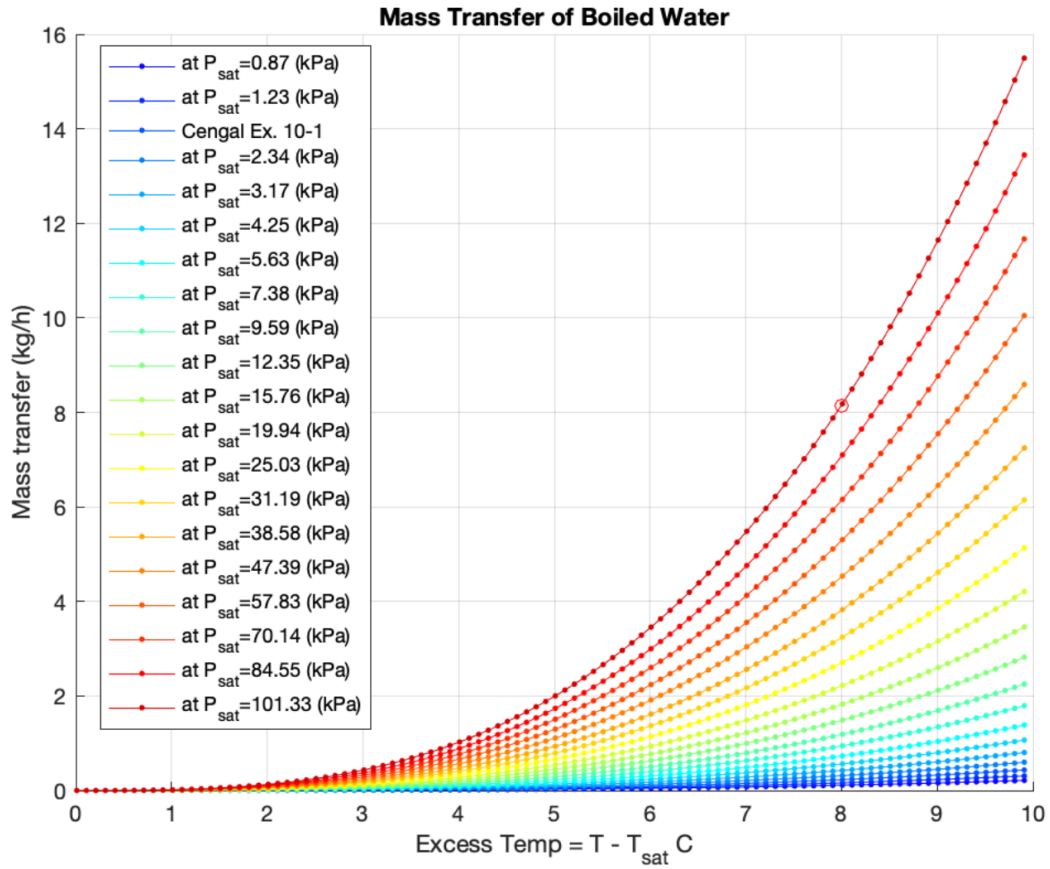


Figure 41: Mass transfer of fresh water vapor as a function of excess temperature.

Figure 41 shows the estimated mass transfer of vaporized water at the range of pressures shown as a function of excess temperature. It is not initially apparent whether or not there are any benefits to lowering the pressure to produce a higher yield of vapor. Figure 41 does however demonstrate that the model is accurate in combination with the Model Validation Points, which are explained below in section 5.4.1.

5.4.1 Model Validation Points

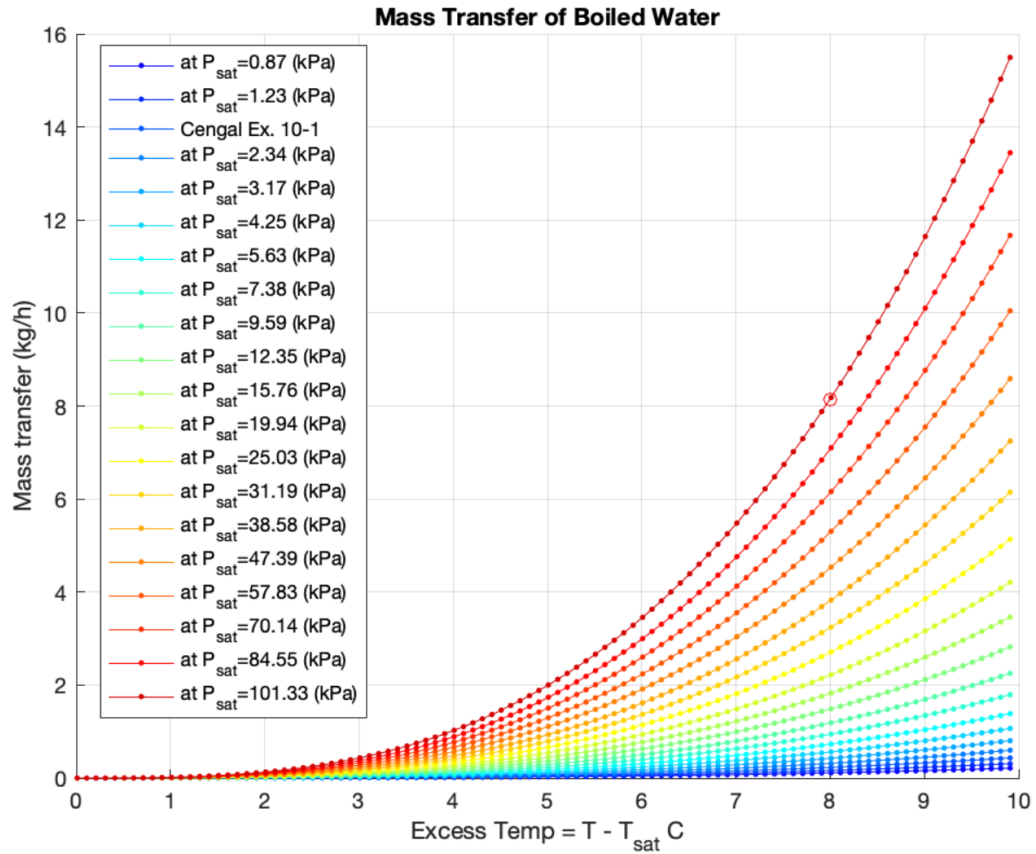


Figure 42: Numerical verification of the math within the model.

The red circle represents an example problem from the textbook Heat and Mass Transfer by Cengel & Gajar. This point on the graph verifies that the math within the model is correct, and that the setup of the code aligns with what would be expected via hand calculations.

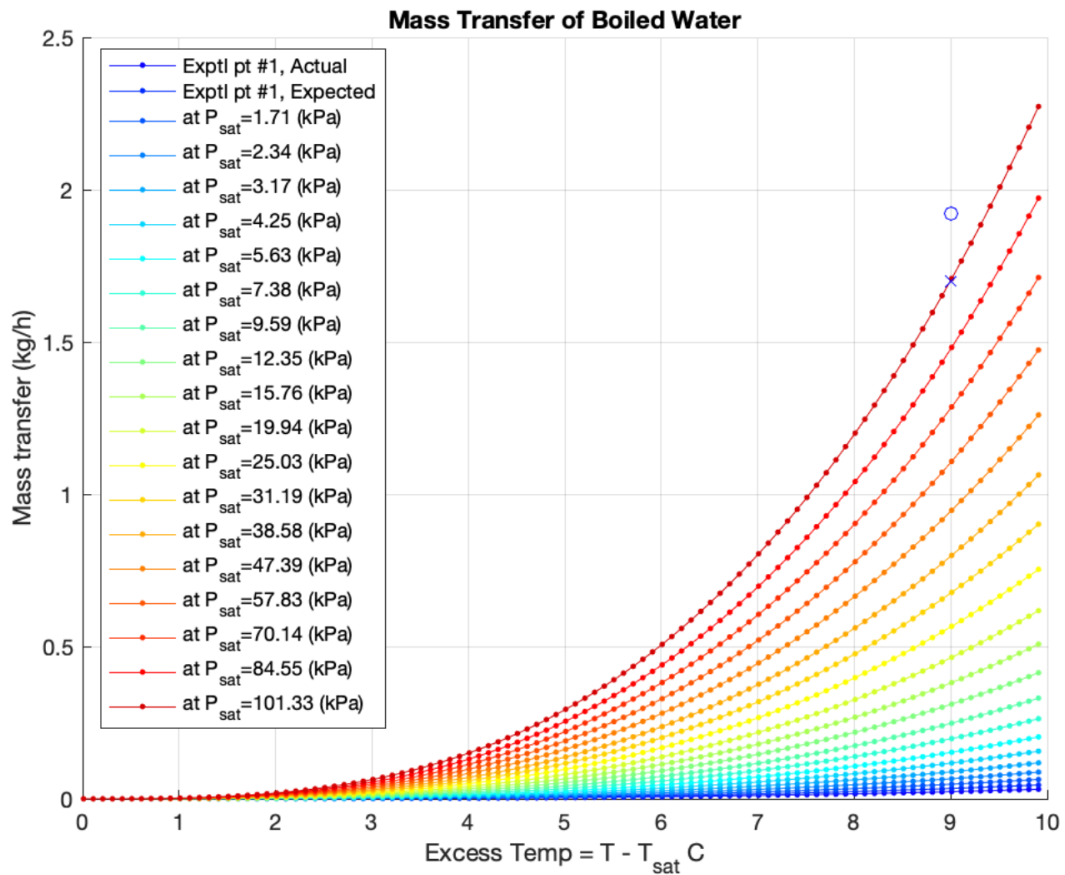


Figure 43: The blue circle represents a physical experimental data point. The blue X shows the predicted point based on the heater surface area.

The blue circle on the graph shows an experimental verification. A physical experiment was conducted to test the model, and at standard pressure, the estimated mass flow rate was where the blue circle lies, very close to the predicted value. The predicted value for the experiment is shown as the blue X.

5.4.2 Estimated Energy Savings for Low Pressure Distillation

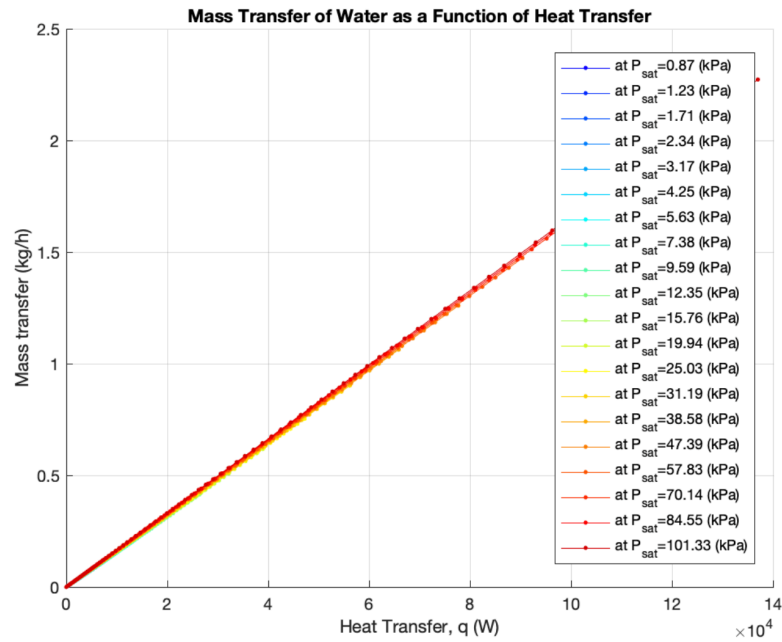


Figure 44: Mass transfer of fresh water vapor as a function of heat transfer.

The above figure demonstrates the relationship between mass transfer of water vapor as a function of heat input. Initially, the results in this figure were disconcerting, as it suggests that lowering the pressure of a system does not actually contribute to heat input savings. The relationship between the heat transfer and mass transfer is defined by the enthalpy of vaporization, so this graph shows that no matter what the pressure is, the relationship between mass transfer and heat input is linear. It is possible that the Rohsenow equation does not accurately predict mass transfer in low pressure scenarios, and this is something that should be experimentally explored and verified.

However, Figure 45 shows that even if is making an accurate prediction, low pressure distillation still offers an opportunity for energy savings. By reducing the sensible heat needed to get the water to vaporization temperature. Once the water is boiling, Figure 44 suggests that it takes the same amount of energy to continue the boil. This means that the energy savings for the system come from what is shown in Figure 45. Reducing the energy needed to get from point (1) to point (3) shows that less heat or energy will be needed to get the system to a boiling point.

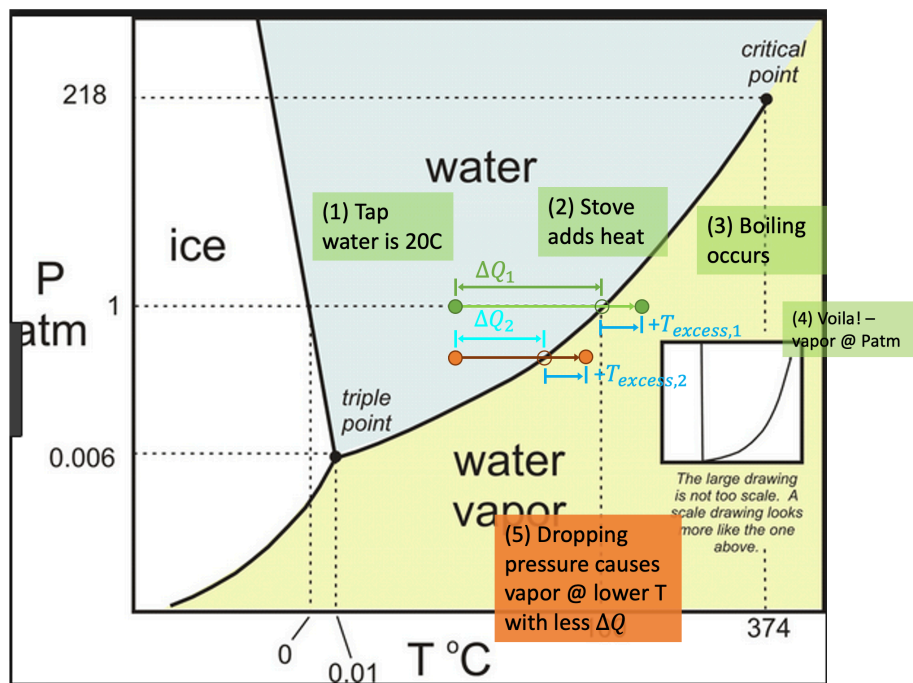


Figure 45: Demonstration of how low-pressure distillation saves energy by reducing the sensible heat needed for the system.

6 Concluding Remarks & Future Work

6.1 Concluding Remarks

In existing literature there is very little information on low pressure boiling, especially in regards to mass transfer. What exists in the literature studies single-phase scenarios for gas or liquid, but not both. Typically, vacuum discussion and analysis is for gases (Fradette & Jones, 2016). Because of the rarity of data on low pressure mass transfer, Rohsenow's model for boiling mass transfer at STP was used to estimate boiling mass transfer at low pressure. This was done by using properties of saturated water in the Rohsenow equation, and then exploring mass transfer, \dot{m} and heat transfer, \dot{Q} for positive excess temperature. Excess temperatures were limited to ensure that the model was within the nucleate boiling zone, which is what the Rohsenow equation was designed for (Cengel & Ghajar, 2016).

Two data points were used to verify the model for boiling at STP using two excess temperatures. The first was both numerically and experimentally verified. The mass transfer rate of boiling water was observed over a time of 12 minutes 30 seconds. The final amount of water in the boiling apparatus was subtracted from the initial amount to estimate change in mass, and this value over time gives the mass transfer rate of vaporized water. This was then numerically calculated and verified. The second data point came from a

textbook example so that another temperature point could verify the mathematics of the model (Cengel & Ghajar, 2016).

Figure 41, Figure 42, and Figure 43 show the required heat transfer and boiling mass transfer rate as a function of excess temperature. The low pressure trend does not initially show favorable results as pressure drops. Figure 44, however, indicates that once the boiling regime starts, the heat transfer and mass transfer do not change as a function of pressure. This indicates that lowering the pressure of the system does reduce heat transfer needed to acquire a certain mass transfer.

Figure 45 is the triple point diagram that clearly indicates a reduced energy requirement to achieve boiling phase change from the same initial temperature. This is a reduction in sensible heat at lower pressures to reach the saturation line and begin the phase change or boiling.

6.2 Future Work

6.2.1 Design of a physical testing apparatus

As mentioned, motion in the bulk fluid increases heat transfer by removing the heated fluid near the surface and replacing it with cooler fluid. Similarly, fluid motion improves mass transfer by “removing the high-concentration fluid near the surface and replacing it by the lower-concentration fluid farther away” (Cengel & Ghajar, 2016). An ideal apparatus should maintain the vacuum within the heating chamber, while inducing

fluid motion. Motion within the fluid encourages heat distribution, while surface motion prevents a high concentration gradient at the surface of the fluid.

The material for the testing apparatus would ideally be very high strength. Operating at such low pressures induces high forces on the boiling chamber. Another consideration is maintaining the vacuum while also allowing for fluid flow in and out of the system in addition to outgoing vapor flow. Check valves could potentially help to allow flow while maintaining vacuum. It will also be important to consider a way to cycle waste water out of the system. Avoiding accumulation of highly concentrated salt water will help to prevent scaling and mineral deposits within the apparatus.

Alternatively to check valves, this process may need to be done in a batch process. In this case, an analysis of the energy savings tradeoff would be imperative, as it may take so much energy to create or maintain the vacuum that it is no longer valuable compared to the thermodynamic savings.

6.2.2 Scalability

As mentioned throughout the paper, a benefit to some desalination methods is the ability to scale the system to meet consumption demands. If low pressure distillation has merit, it is unclear at this point if it would be best suited in small-scale situations such as the solar dome, or if it has the potential to be scaled up to produce municipal scale fresh water. Once a physical apparatus for testing is designed, it would be valuable to explore how large a low pressure system could be while being economically competitive.

6.2.3 *Standard Test Procedure*

Currently, there is not a standard test procedure for this process. It would be valuable to explore the energy requirements and performance of brackish water versus salt water. It will also be important to test the salinity of the collected fresh water. It is possible for salt molecules to contaminate the fresh water, so maintaining saline levels below recommended guidelines will be an important step in the testing and development process.

6.2.4 *Experimental Verification of Rohsenow at Low Pressure*

The Rohsenow equation was developed from the conglomeration of data on boiling phenomenon (Cengel & Ghajar, 2016). It is not known if any of this experimentation was done at low pressure. It will be important to experimentally verify the Rohsenow equation at low pressure, as it currently is the best model available to relate heat transfer, temperature, and vapor mass transfer. For the sake of the model in this paper, it was assumed that if the temperature of the water is above the vaporization temperature at the given pressure, the water would be in the nucleate boiling phase and thus Rohsenow could apply.

It should also be explored whether the enthalpy of vaporization accurately reflects the relationship of heat transfer and mass transfer at low pressure. It was indicated that there is not a reduced energy to maintain the boiling regime at low pressure. It seems that

if it takes less energy to achieve phase change, it will also require less energy to sustain the boiling regime. This may be proven wrong but should be explored.

6.2.5 Energy trade off: drawing vacuum versus thermodynamic energy savings

Finally, it will be valuable to analyze the energy trade-off for drawing a vacuum versus the energy saved for low pressure vaporization. It is unclear if the energy savings of lowering the pressure would be valuable when compared to the cost of the energy to achieve low pressure within a system. Depending on the physical design of the boiling system, the vacuum may be self-sustaining, meaning that the system will require the initial energy input to create the vacuum but then little to sustain it. If the system has leaks, it will be important to consider how much energy it takes to sustain the low pressure environment. The quality of the vacuum (or how low the pressure is set) will also matter in the calculations of energy cost of the low pressure environment. Once these parameters are understood, a thermo-economic analysis of the system will increase the understanding of whether low pressure distillation stands as a meaningful contribution to desalination and global water security.

7 Referencess

- Ahsan, A., & Fukuhara, T. (2010, March 21). Mass and heat transfer model of Tubular Solar Still. *Solar Energy*, 84, 1147-1156.
- Al-Karaghoul, A., Kazmerski, L. L., & (NREL). (2013, August). Energy consumption and water production cost of conventional and renewable-energy-powered desalination processes. *Renewable and Sustainable Energy Reviews*, 24, 343-356.
- Aultman, W. W. (1949, February). Fresh Water From Salt. *Engineering and Science Monthly*, XII(5), 3-7.
- Bergman, T., Incropera, F., DeWitt, D., & Lavine, A. (2011). *Fundamentals of Heat and Mass Transfer*. John Wiley & Sons.
- Boretti, A., Al-Zubaidy, S., Vaclavikova, M., Al-Abri, M., Castelletto, S., & Mikhalovsky, S. (2018). Outlook for graphene-based desalination membranes. *npj Clean Water*.
- Borgen, M. (2019). *United states : Costa crociere foundation and sahara forest project join forces for sustainable farming in the desert of jordan*. London: MENA Report.
- Cengel, Y. A., & Ghajar, A. J. (2016). *Heat and Mass Transfer; Fundamentals and Applications*. McGraw Hill.

- Chandrasekharam, D., Lashin, A., Arifi, N. A., Al-Bassam, A. M., & Varun, C. (2019, June). Geothermal energy for desalination to secure food security: case study in Djibouti. *Energy, Sustainability, and Society*, 9(1), 1-11.
- Chandrasekharam, D., Lashin, A., Arifi, N., Al Bassam, A., & Varun, C. (2017, Feb). Desalination of Seawater using Geothermal Energy to Meet Future Fresh Water Demand of Saudi Arabia. *Water Resources Management*, 31(3), 781-792.
- Cho, R. (2011, February 18). *Seawater Greenhouses Produce Tomatoes in the Desert*. Retrieved from State of the Planet:
<http://blogs.ei.columbia.edu/2011/02/18/seawater-greenhouses-produce-tomatoes-in-the-desert/>
- Chu, J. (2018, April 17). *A graphene roll out: scalable manufacturing process spools out strips of graphene for use in ultrathin membranes*. Retrieved from MIT News.
- Cohen, Y., Semiat, R., & Rahardianto, A. (2017). A perspective on reverse osmosis water desalination: Quest for sustainability. *AIChE Journal*, 63(6), 1771-1784.
- Cohen, Y., Semiat, R., & Rahardianto, A. (2017, June). A Perspective on reverse osmosis water desalination: quest for sustainability. *AIChE Journal*, 63(6), 1771-1784.
- Cohen, Y., Semiat, R., & Rahardianto, A. (2017). A Perspective on Reverse Osmosis Water Desalination: Quest for Sustainability. *American Institute of Chemical Engineers*, 1771-1784.

- Cooper, P. (1973). The maximum efficiency of single-effect solar stills. *Solar Energy*, 3, 205-217.
- Crain, J., Oropeza, I., Divo, E., Kassab, A. J., & Narayanan, R. (2006). Oscillatory flow as a means of enhanced species separation: a three-dimensional time-accurate numerical study. Florida, USA: University of Florida.
- Critical point vs. Triple point: what's the difference?* (n.d.). Retrieved from Vivadifferences: <https://vivadifferences.com/difference-between-critical-point-and-triple-point/>
- Del Valle M, V. H., & Kenning, D. (1985). Subcooled flow boiling at high heat flux. *International Journal of Heat Mass Transfer*, 1907-1920.
- Department of International Economic and Social Affairs, U. N. (1992). *Long-Range World Population Projections: Two Centuries of Population Growth 1950-2150*. United Nations.
- El Kadi, K., & Janajreh, I. (2017). Desalination by Freeze Crystallization: an Overview. *International Journal of Thermal & Environmental Engineering*, 15, 103-110.
- Elimelech, M., & Phillipl, W. A. (2011, August 05). The Future of Seawater Desalination: Energy, Technology, and the Environment. *Science*, 333(6043), 712-717.
- Faghri, A., & Zhang, Y. (2006). *Transport Phenomena in Multiphase Systems*.
- Feher, J. (2017). *Quantitative Human Physiology*. Elsevier Inc.

- Fouda, A., & Melikyan, Z. (2010). A simplified model for analysis of heat and mass transfer in a direct evaporative cooler. *Applied Thermal Engineering*, 932-936.
- Fradette, R. J., & Jones, W. R. (2016). *Understanding Vacuum and Vacuum Measurement*. Solar Manufacturing.
- Giraud, F., Rulliere, R., Toublanc, C., Clause, M., & Bonjour, J. (2015). Experimental evidence of a new regime for boiling of water at subatmospheric pressure. *Experimental Thermal Fluid Science*, 60, 45-53.
- Glater, J. (1998). The early history of reverse osmosis membrane development. *Desalination*, 279-309.
- Glensvig, M., Stowe, C., & Schutting, E. (2013). Method for active EGR cooler refreshing during cold start. *Vehicle Thermal Management Systems Conference Proceedings*, 65-77.
- Hanasaki, N., Fujimori, S., Yamamoto, T., Yoshikawa, S., Masaki, Y., & Hijioka, Y. (2013, July 1). A global water scarcity assessment under Shared Socio-economic Pathways -- Part 2: Water availability and scarcity. *Hydrology and Earth System Sciences*, 17(7), p. 2393.
- Hawllader, M., & Liu, B. (2002). Numerical study of the thermal-hydraulic performance of evaporative natural draft cooling towers. *Applied Thermal Engineering*, 22, 41-59.

- How Solar Stills Work*. (2012, November 13). Retrieved from TurbineGenerator:
<https://www.turbinegenerator.org/how-a-solar-stills-works/>
- Jones, E., Qadir, M., van Vliet, M., Smakhtin, V., & Kang, S.-m. (2019, March 20). The state of desalination and brine production: a global outlook. *Science of the Total Environment*, 657, 1343-1356.
- Kennedy, E. B. (2017). Biomimicry: Design by Analogy to Biology. *Research-Technology Management*, 51-56.
- Lee, J., & Mudawar, I. (2009). Critical heat flux for subcooled flow boiling in micro-channel heat sinks. *International Journal of Heat and Mass Transfer*, 52, 3341-3352.
- Lee, K. P., Arnot, T. C., & Mattia, D. (2010). A review of reverse osmosis membrane materials for desalination-Development to date and future potential. *Journal of Membrane Science*.
- Lovette, I. J., & Fitzpatrick, J. W. (2017, June 6). *Why Can Some Birds Drink Salty Seawater?* (Cornell University) Retrieved 2020, from The Cornell Lab.
- Mazlan, M. N., Peshev, D., & Livingston, A. (2016). Energy consumption for desalination — A comparison of forward osmosis with reverse osmosis, and the potential for perfect membranes. *Desalination*, 377, 138-151.

- McGillis, W. R., & Carey, V. P. (1991). Pool Boiling Enhancement Techniques for Water at Low Pressure. *1991 Proceedings, Seventh IEEE Semiconductor Thermal Measurement and Management Symposium*.
- McGillis, W., Carey, V., Fitch, J., & Hamburgren, W. (1991). Pool boiling on small heat dissipating elements in water at subatmospheric pressures. Minneapolis, Minnesota.
- Michaie, S., Rulliere, R., & Bonjour, J. (2019). Towards a more generalized understanding of pool boiling at low pressure: Bubble dynamics for two fluids in states of thermodynamic similarity. *Experimental Thermal and Fluid Science*, 217-230.
- Newton, D. E. (2011). "Geothermal Energy". In Gale, *Environmental Encyclopedia, 4th ed.* (Vol. 1, pp. 753-756). Detroit, MI: Gale eBooks.
- Niro, A., & Beretta, G. (1990). Boiling Regimes in a Closed Two-Phase Thermosyphon. *International Journal of Heat and Mass Transfer*, 2099-2110.
- NOAA (National Oceanic and Atmospheric Administration). (2004, December 16). *National Ocean Service*. Retrieved from National Oceanic and Atmospheric Administration: <https://oceanservice.noaa.gov/facts/oceanfreeze.html>
- Okamoto, Y. (2019). How RO membrane permeability and other performance factors affect process cost and energy use: A review. *Desalination*, 470-475.

- Okamoto, Y., & Leinhard, J. (2019). How RO membrane permeability and other performance factors affect process cost and energy use: A review. *Desalination*, 470, 114064.
- Patel, J., Markam, B. K., & Maiti, S. (2019). Potable water by solar thermal distillation in solar salt works and performance enhancement by integrating with evacuated tubes. *Solar Energy*, 188, 561-572.
- Ponter, A., & Haigh, C. (1969). Sound emission and heat transfer in low pressure pool boiling. *International Journal of Heat and Mass Transfer*, 12(4), 413-428.
- Ponter, A., & Haigh, C. (1969). The boiling crisis in saturated and subcooled pool boiling at reduced pressures. *International Journal of Heat and Mass Transfer*, 12(4), 429-437.
- Pugsley, A., Zacharopoulos, A., Mondol, J., & Smyth, M. (2016). Global applicability of solar desalination. *Renewable Energy*, 88, 200-219.
- PureRO USA. (2019). *PurePro USA Nanofiltration (NF) Membranes*. Retrieved from PurePro Drinking Water System: https://www.purepro.com/purepro_membrane.htm
- REVE. (2013, June 13). *Tap geothermal energy for water desalination*. Retrieved from REVE - Wind Energy and Electric Vehicle Review.
- Rohsenow, W. (1952). A Method of Correlating Heat Transfer Data for Surface Boiling of Liquids. *Transactions, ASME*, 74.

- Rosa, A. V. (2013). *Fundamentals of Renewable Energy Processes 3e*. Elsevier.
- Sahara Forest Project*. (n.d.). Retrieved from Jordan:
<https://www.saharaforestproject.com/jordan/>
- Schnabel, L., Scherr, C., & Weber, C. (2008). Water as refrigerant - experimental evaluation of boiling characteristics at low temperatures and pressures. *International Sorption Heat Pump Conference*. Seoul, Korea.
- Sengupta, S., & Cai, W. (2019, August 6). *A Quarter of Humanity Faces Looming Water Crises*. Retrieved from The New York Times.
- Shiklomanov, I. A. (1993). World fresh water resources. Water in crisis: a guide to the World's fresh water resources. *Oxford University Press*, 13-24.
- TWI. (2021). *What are Technology Readiness Levels? (TRL)*. Retrieved from TWI Global: <https://www.twi-global.com/technical-knowledge/faqs/technology-readiness-levels>
- Ullah, A., Shahzada, K., Khan, S. W., & Starov, V. (2020, October 1). Purification of produced water using oscillatory membrane filtration. *Desalination*, 491.
- United Nations. (2020). *The 17 Goals*. Retrieved from United Nations Department of Economic and Social Affairs: <https://sdgs.un.org/goals>
- Van Stralen, S., Cole, R., Sluyter, W., & Sohal, M. (1975). Bubble growth rates in nucleate boiling of water at subatmospheric pressures. *International Journal of Heat and Mass Transfer*, 18, 655-669.

- Veerapaneni, S., Long, B., Freeman, S., & Bond, R. (2007, June). Reducing energy consumption for seawater desalination. *American Water Works Association*, 99(6), 95.
- Vorosmarty, C. J., Green, P., Salisbury, J., & Lammers, R. B. (2000, July). Global Water Resources: Vulnerability from Climate Change and Population Growth. *Science*, 289, 284-288.
- Wang, G., & Cheng, P. (2009). Subcooled flow boiling and microbubble emission boiling phenomena in a partially heated microchannel. *International Journal of Heat and Mass Transfer*, 52, 79-91.
- WWAP (UNESCO World Water Assessment Programme). (2019). *The United Nations World Water Development Report 2019: Leaving No One Behind*. Paris: UNESCO.
- Yan, J., Bi, Q., Lui, Z., Zhu, G., & Cai, L. (2015). Subcooled flow boiling heat transfer of water in a circular tube under high heat flux and high mass fluxes. *Fusion Engineering and Design*, 406-418.
- Yeang, K., & Pawlyn, M. (2009). Seawater Greenhouses and the Sahara Forest Project. In J. W. Ltd., *Exploration Architecture* (p. 122).
- Zaal, C., Daniilidis, A., & Vossepoel, F. C. (2021, April). Economic and fault stability analysis of geothermal field development in direct-use hydrothermal reservoirs. *Geothermal Energy*, 9(1).

Zajackowski, B., Halon, T., & Krolicki, Z. (2016). Experimental verification of heat transfer coefficient for nucleate boiling at sub-atmospheric pressure and small heat fluxes. *Heat and Mass Transfer*, 52, 205-215.

Zhang, X., Dai, Y., & Wang, R. (2003). A simulation study of heat and mass transfer in a honeycombed rotary desiccant dehumidifier. *Applied Thermal Engineering*, 23, 989-1003.